THESIS FOR THE DEGREE OF LICENTIATE OF ENGINEERING

Phase Dependent Heat Transport in Superconducting Junctions with Scattering Theory

FATEMEH HAJILOO

Department of Microtechnology and Nanoscience (MC2)
Applied Quantum Physics Laboratory
CHALMERS UNIVERSITY OF TECHNOLOGY

Göteborg, Sweden 2018

Phase Dependent Heat Transport in Superconducting Junctions with Scattering Theory
FATEMEH HAJILOO

Thesis for the degree of Licentiate of Engineering
ISSN 1652-0769
Technical Report MC2-331

Applied Quantum Physics Laboratory
Department of Microtechnology and Nanoscience (MC2)
Chalmers University of Technology
SE-412 96 Göteborg
Sweden
Telephone: +46 (0)31-772 1000

Cover
Sketch of a hybrid junction across which a temperature bias is applied; transport of quasiparticles from hot to cold occurs through a disordered central region. Desighned with the help from Leila Hajiloo.

Printed by Chalmers Reproservice
Göteborg, Sweden 2018

Phase Dependent Heat Transport in Superconducting Junctions with Scattering Theory
Thesis for the degree of Licentiate of Engineering

FATEMEH HAJILOO

Department of Microtechnology and Nanoscience (MC2)
Applied Quantum Physics Laboratory
Chalmers University of Technology

Abstract

The operation of nanoscale devices at low temperatures is highly sensitive to heating effects. This motivates current research on controlling heat currents in these devices. A particularly important class of setups are hybrid superconducting devices, since (1) there exist a variety of sensitive applications such as qubits, in which heating is an issue, and (2) because the superconducting energy gap as well as the controllable phase-difference across junctions allow for cooling and heat control.

This thesis deals with phase-controllable heat currents through superconducting-normal conducting-superconducting (SNS) Josephson junctions. Elaborate devices containing junctions of this type have in recent years been proposed and partly even experimentally been implemented in heat interferometers, heat switches and heat diodes. These complex structures motivate our study on how the properties of an extended, diffusive junction affect the phase-dependent heat conductance of SNS Josephson junctions. In order to analyse the heat conductance of such junctions, in which heat is carried by quasiparticle excitations of the superconducting condensate, we use a scattering matrix formalism for hybrid superconducting systems. The transmission of quasiparticles through the diffusive region takes place via a large number of transmission channels with transmission probabilities characterized by a statistical distribution. We implement these statistical properties using previously obtained results from random-matrix theory. Our main findings are that the channel average of the diffusive conductor leads to a full suppression of the phase-dependence of the heat conductance. In contrast, the weak-localization correction to the heat conductance, as well as the heat conductance fluctuations are still sensitive to the phase. We also find that these heat conductance fluctuations have a similarly universal behavior as the well-known conductance fluctuations of charge currents in normal conductors. However, we identify an additional non-trivial temperature dependence, which is due to the superconducting phase difference.

Keywords: heat transport; superconducting hybrid devices; scattering theory; phase dependent heat currents; heat conductance; conductance fluctuations.

Acknowledgements

First and foremost, I would like to thank my lively, enthusiastic and energetic supervisor Janine Splettstoesser. I am proud of working with you. Thank you for giving me this opportunity and thank you for your unlimited and invaluable supervision. You have changed my viewpoints entirely to a supervisor. You guided me with patience, and I am grateful to all the trust you showed me. My research would have been impossible without all your aids. I would also like to thank you for being a friend with me, and for all the nice moments we had together.

I am grateful to my co-supervisor, Fabian Hassler at RWTH Aachen University. I had a very productive time during my visit in Aachen which all comes from your help. Thank you for encouraging my research and for your hospitality.

I would like to thank Maciej Misiorny and Jens Schulenborg for their valuable help. Thank you for all the time you spent in discussions with me and giving feedback to my research and thank you for being kindly available whenever I needed your help. I wish you the best. I would also like to thank Angelo Di Marco for helpful discussions we had at the beginning of my research.

I would especially like to thank my friend Nastaran Dashti. You are a great friend and colleague. Words cannot express my feelings to you. Thank you for the helpful discussions and your company.

I thank Mohammadamir Ghaderi for helping me to learn useful softwares in my work.

My heartfelt thanks go to all previous and present members in Applied Quantum Physics group at MC2 for all the beautiful moments you made for me. Special thanks to my officemates for their kindness and patience. I thank my friends in quantum Device Physics and Quantum Technology groups for their company.

My time at Chalmers was made enjoyable in large part due to my Iranian friends here. I am grateful for the time spent with all of you.

I thank Chalmers Karateklubb members and my sensei, Per Lundgren.

Last, by no means least, I would like to thank my family for their constant support and unconditional love.

List of figures

Contents

1 Introduction

In this thesis we study thermal effects in nano-scale devices. The operation of nano-scale devices at low temperatures is sensitive to heating effects. This motivates the study on controlling heat currents in these devices.

One class of particularly relevant nano-scale devices are setups containing superconducting elements, since heat transport in such junctions is remarkably influenced by the specific characteristics of superconductivity [1, 2]. One of these characteristics is the superconducting temperature-dependent energy gap. The energy gap makes superconductors good energy filters, in the sense that they only allow quasiparticles (constituting the energy carriers in superconductors) at specific energies to tunnel out from or into an electrode. Depending on the device operation this makes the superconducting electrode or closeby normalconductors to be cooled [3]. Therefore having superconducting elements as part of hybrid systems is useful for cooling: it allows for an implementation of electronic refrigerators [1], thereby improving the performance of electronic devices.

However, in this thesis, the focus is on superconducting junctions used as heat rectifiers and heat current switches [4, 5]. Here, another aspect of superconductors plays the most important role, namely the possibility of heat current control via the phase-dependence of superconducting junctions. It has been theoretically predicted [2] that heat currents through so-called Josephson junctions, consisting of two superconductors separated by an insulator (SIS), depend on the relative phase of the superconducting condensates of the two superconducting regions. This theoretical work has been generalized and refined in several follow-up works [6–8]. Only, a few years ago, this intriguing effect has also been proven experimentally [5, 9]. Since then, various different devices, which exploit this effect for heat current-control, have been proposed and partially even implemented experimentally, see [10] for a recent review.

These developments motivate theoretical studies on how phase-dependent heat transport depends on the properties of possibly complex hybrid (normal(N)- and superconducting(S)) junctions. The focus of this work is on junctions, consisting of extended diffusive conductors, in which many transport channels with randomly distributed transmission probabilities can contribute to heat transport via quasiparticles. The impact of these trasnmission statistics on the phase-dependent thermal conductance have not been considered so far.

In order to approach the role of complex junction properties on heat transport, in this Licentiate thesis, we elaborate a formalism to study heat transport in

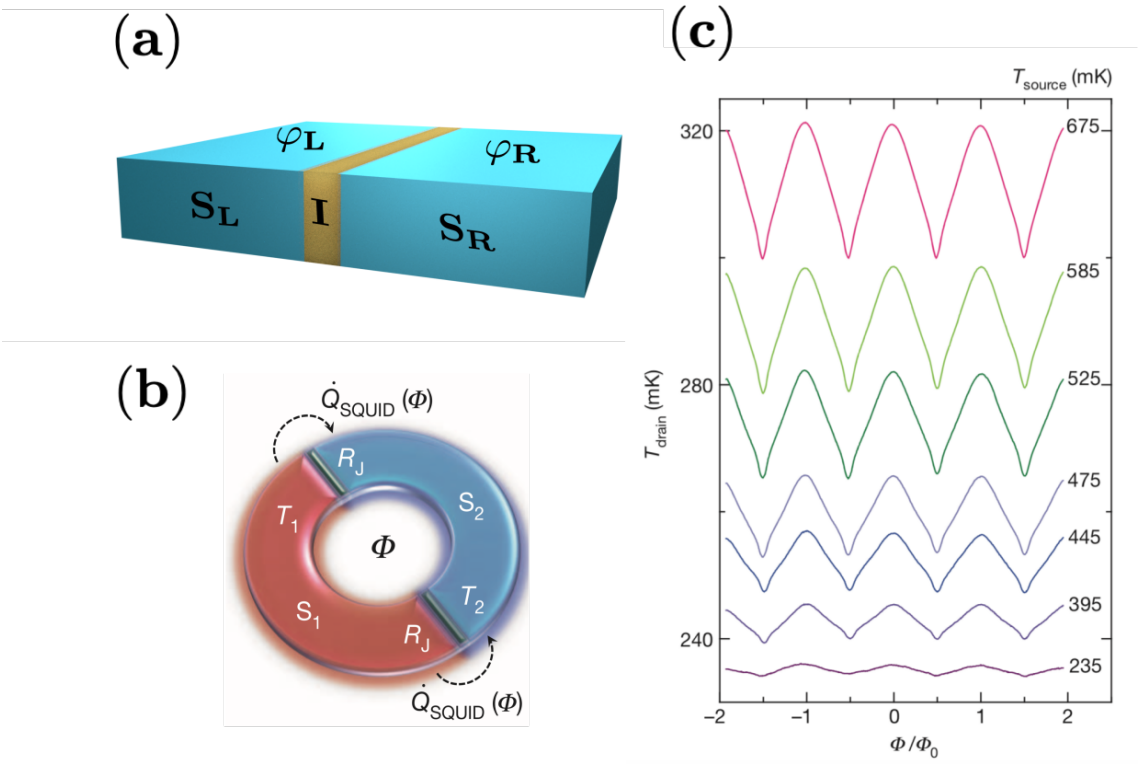

Figure 1.1: *(a) Structure of a Josephson junction with two superconductors with different phases φ_L, φ_R. (b) Scheme of a temperature biased SQUID made of two identical superconductors S1 and S2. Temperature T_1 is kept fixed, while the temperature $T_2 < T_1$ is influenced by the heat flow across the junctions. R_J is the normal state resistance of each junction and $\dot{Q}_{SQUID}(\Phi)$ is the heat current flowing from the hotter to the colder superconductor. (c) Flux modulation of the drain temperature $T_{drain} \equiv T_2$ of the superconductor S_2 in the structure shown in (b) [9].*

superconducting hybrid devices which is based on a scattering matrix approach. In contrast to powerful, but complex Green's function approaches for electron- and hole-like quasiparticle excitations, which have been employed in the seminal theoretical works on this topic [2, 6–8], the scattering approach allows to straightforwardly implement different types of junction properties. We use this both for the theoretical description of the above-mentioned heat-conductance statistics of diffusive SNS junctions, but also for heat conductance calculations of NS junctions, which are often used to suppress detrimental effects of hot quasiparticles in superconductors [11]. Furthermore, we envision to exploit this approach for the study of heat currents, or even of heat current noise, in junctions with differently designed structures in the future.

In addition to the practical interest in heat current control in superconducting devices specifically, there is however an even broader interest in heat currents in generic phase-coherent setups. Recently, the field of *quantum thermodynamics*,

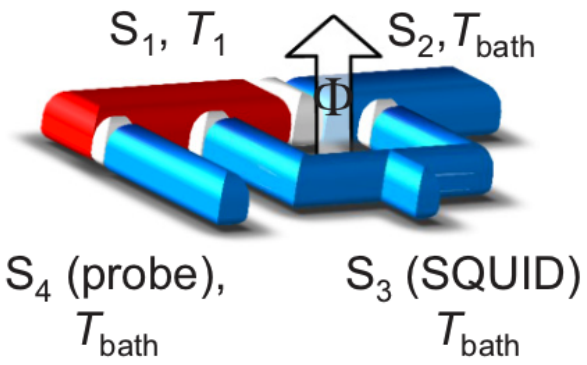

Figure 1.2: *Phase-biasing a Josephson junction by means of a three-junction SQUID [18].*

combining the apparently distinct thermodynamical properties of quantum- and nanoscale systems and statistically described macroscopic systems, has gained a lot of interest. In this context, for example, quantum heat engines have been theoretically studied [12–14]. Furthermore, the possibility of enhancing the efficiency of thermoelectric devices using quantum effects, for heat to electricity conversion and also energy harvesting [15–17], is currently addressed. Also in this broader context, the theoretical results of this Licentiate thesis are expected to be of interest.

1.1 Heat transport in hybrid superconducting devices

Generally, electronic transport happens together with transport of energy and therefore of heat.[1] Our aim is to study *phase-coherent* heat transport in superconducting hybrid devices.

Hybrid devices are structures which contain superconducting elements as well as normal conductors or insulators. We concentrate on Josephson junctions—structures containing two superconductors connected by an insulator (SIS) or a small normal metal conductor (SNS). Transport across Josephson junctions is governed by the phase difference between the two superconducting condensates of the junction. Indeed, Josephson junctions form the basis of an extensively used device, the superconducting quantum interference device (SQUID) [19]. In panel (a) of Fig. (1.1) we show a schematic representation of a Josephson junction. The phase difference of the two superconducting leads results in a *dissipationless* charge current in the absence of any bias voltage. This charge current is carried by Cooper pairs, $I = I_c \sin\varphi$. This famous effect is known as the Josephson effect

[1] Note that we do not treat heat transport due to phonons or photons, which in shielded low-temperature devices as the ones considered here is suppressed.

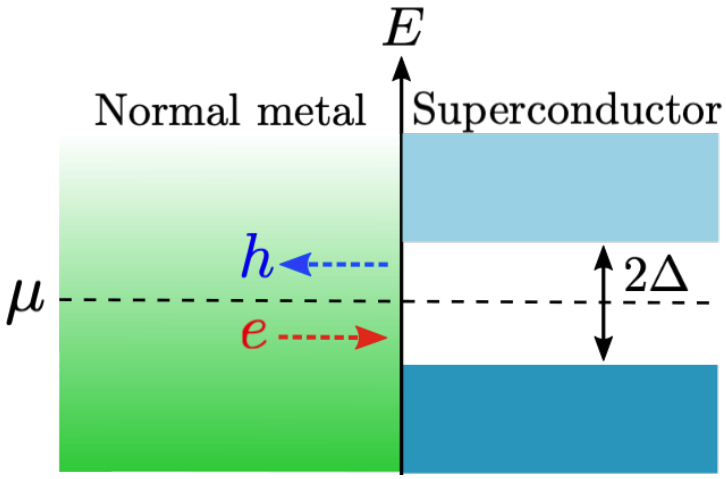

Figure 1.3: *Subgap Andreev reflection: An electron incoming to an NS interface from the normal-conducting side is reflected as a hole, while a total charge of* $2e$ *is transmitted into the superconductor. Equivalently, quasiparticles above the superconducting gap can be Andreev-reflected.*

and has first been predicted by Brian Josephson [20]. Importantly, this current flows in the absence of any heat current!

However, when a temperature bias is applied between the two superconducting leads, there will be a heat current flowing through the junction. This heat is carried by electron- and hole-like quasiparticle excitations that exist in the superconductors at energies above the superconducting gap, when the temperature of these leads are different from zero. A striking property of this heat current is its dependence on the phase difference of the two superconducting condensates, as predicted by Maki and Griffin [2]. The phase-dependent transport of quasi-particles arcoss the junction takes place via Andreev reflection at the superconductor's interface. The Andreev reflection is a type of particle scattering which occurs at the interfaces between a superconductor and a normal conductor and consists in a back reflection of, e.g., an electron-like quasiparticle into a hole by transferring a charge of $2e$ to the superconductor [21]. In Fig. (1.3) Andreev reflection is schematically shown, for an NS junction at an energy, where normal single-particle transmission is forbidden due to the superconducting gap. Note however, that for the heat current considered here, also Andreev reflection *above* the gap is relevant.

Only recently, this phase-dependence of the quasiparticle heat current across a Josephson junction has been proven experimentally [9]. In Figs. (1.1) and (1.2), we show schematic sketches of the setup and the results of this experimental realization. The basic ingredient of the experiment is a three-junction SQUID, see Fig. (1.2), which allows for a modulation of the superconducting phase-difference via an applied magnetic flux. One of the SQUID segments is heated to a fixed temperature T_1. The quasi-particle heat flow across the junction results in a

measurable temperature change on the other side of the junction, T_2. Due to the phase-dependence of the heat current, also the resulting temperature change is phase dependent. This can be seen in Fig. (1.1c).

The phase-dependent control of heat currents has been the basis for a number of experimental proposals and realizations: by biasing different phases in similar setups even the directions of heat currents can be controlled, resulting in the experimental design of a heat diode, and different designs of thermal transistors, which might operate as a thermal switch or as an amplifier/modulator [10].

1.2 Heat conductance

In order to focus on the study of the fundamental heat transport properties of an SNS junction, we consider the heat conductance, namely the linear response to the temperature gradient. This quantity is furthermore of relevance for realistic situations, where the temperature gradient is not intentional, but results from the operation of a device [22]. Then one expects the case when the temperature difference of the two superconducting leads is very small, $T_{\mathrm{L}} = T$ and $T_{\mathrm{R}} = T+\delta T$, with $\delta T \ll T$.

We are interested in how the properties of the junction influence this phase-dependent linear-response heat conductance. More specifically, we focus on a situation where the normal-conducting segment connecting the two superconductors is diffusive and of a finite length $\mathcal{L}$. This diffusive normal conductor supports $\mathcal{N}$ transport channels. In order to consider the effect of these many channels, which contribute to transport with randomly distributed transmission probabilities, we take an average of the heat conductance over all these channels using the DMPK formalism [23]. This formalism suggests a distribution of transmissions in the normal metal which depends on the junction length. It is valid in the length scales where the junction length is much smaller than the localization length of electrons (short junction limit) and much larger than the mean free path of electrons (diffusive regime). More details about the formalism and the resulting averaged heat conductance are discussed in Section 3.2. The main finding here is that the averaging *fully suppresses* the phase-dependence of the heat conductance, which has major consequences for the requirements on the device design of coherent heat modulators. Interestingly, the weak-localization correction to the conductance remains however phase-dependent.

1.3 Heat conductance fluctuations

After studying the heat conductance considering many transport channels for an SNS junction, we study the behavior of heat conductance fluctuations in superconductors and the influence of phase difference on it.

The research on conductance fluctuations of the charge current in diffusive conductors caught attention already decades ago. Most interestingly, it was found that these conductance fluctuations can be universal (UCF). This was first theoretically discovered in 1985 by Altshuler, and Lee and Stone [24, 25] and has been observed in many experiments [26]. The conductance fluctuations are universal from two aspects. One is that the order of magnitude of the variance of the conductance (or in other words the conductance fluctuations) normalized to the quantum of conductance, $G_0 = 2e^2/h$, is of order unity

$$\mathrm{Var}\left[\frac{G}{G_0}\right] \simeq 1 \ . \tag{1.1}$$

On the other hand, the conductance fluctuations is weakly dependent on the shape of the conductor. This means, more specifically, that Var$[G]$ neither depends on the length of the junction $\mathcal{L}$, nor on the number of transverse modes $\mathcal{N}$. Only the symmetry class modifies the value of the UCFs (e.g., the fluctuations in a system with or without time-reversal symmetry breaking differ by a factor of 2).
One explanation for UCF was put forward by Imry [27] using an argument based on the number of open scattering channels which contribute effectively to the conductance. In a disordered conductor most transmission eigenvalues are exponentially small, implying that those channels are closed. A fraction $l/\mathcal{L}$ (where l is the mean free path) of the total number $\mathcal{N}$ of transmission eigenvalues is of order unity—these channels are open. Only open channels contribute to the conductance. Therefore the effective number of channels is $\mathcal{N}_{\mathrm{eff}} \approx \mathcal{N}l/\mathcal{L}$.
Universal conductance fluctuations originate from quantum fluctuations. The reason for that is that on length scales below the phase coherence length, L_φ (namely the distance across which the electrons loose phase memory), interference effects are important and interference is sensitive to the disorder in a given system. Therefore it can generate fluctuations, stemming from certain interfering paths only. The aim of this work is to study the effects of these fluctuations on the heat conductance.
In normal metals, the conductance fluctuations of the heat conductance are not of special interest; the transmission of transport channels contributes to the electrical conductance basically in the same way as to the thermal conductance. Therefore thermal conductance fluctuations are expected to have similar properties, except for an overall prefactor depending quadratically on the temperature of the system. More concretely, for the heat conductance κ_{N} of a fully normal-conducting junction, we can write

$$\mathrm{Var}\left[\frac{\kappa_{\mathrm{N}}}{\kappa_0}\right] \simeq 1 \tag{1.2}$$

where $\kappa_0 = \frac{\pi^2 k_{\mathrm{B}}^2}{3h} T$ is the temperature-dependent heat conductance quantum.

This is different in Josephson junctions, consisting of two superconductors connected by a normal-conducting junction (SNS). In such a highly nonlinear device, the linear conductance G is zero. The linear *heat* conductance κ_{SNS} is however finite [2] and has recently attracted interest due to its phase-dependent properties [7–9]. The study of heat conductance fluctuations in such systems is however lacking.
In Chapter 3 we study the heat conductance fluctuations in an SNS junction using the DMPK formalism. We find that the heat conductance fluctuations remain universal, in the sense that their magnitude is independent of the specific shape and size of the conductor. We can however identify an interesting temperature-dependence, which is different from the temperature-dependence of a normal setup and which is related to the phase-dependence of κ_{SNS}.

1.4 Scattering theory

The theoretical approach used in the above mentioned theoretical works on phase-dependent heat currents is mostly based on Green's function methods, which can be demanding particularly when the system to be studied gets complex itself. This motivates us to use a more straight forward method to study heat transport which is scattering theory. In particular, for the calculation of average heat conductances in diffusive conductors, its weak localization corrections, as well as conductance fluctuations, based on previously obtained results from random matrix theory [23], the scattering matrix approach turns out to be most appropriate.

The scattering theory of electronic transport in mesoscopic conductors was first developed by Landauer and Büttiker [28–30]. It is most applicable for systems in which the many-body interaction between quasiparticles is negligibly small. In Chapter 2 a general model of a nanostructure is shown, in which a picture of single-particle transport is visualized, see Fig. (2.1). There is a scattering region connected to reservoirs via perfect leads. A particle flux coming in from the equilibrium reservoirs is scattered at the central region. This is described by a scattering matrix, which relates the incoming to outgoing fluxes to the scatterer

$$\vec{b} = S\vec{a}. \tag{1.3}$$

The scattering matrix S is a unitary matrix, $S^{-1} = S^{\dagger}$, guaranteeing current conservation at the scatterer. We here assume that particle scattering happens without energy loss, in other words it is elastic. The transmission amplitudes entering the scattering matrix, as well as the resulting transmission probabilities govern the charge and heat current through a junction, which we are interested in.

Charge transport in superconducting hybrid systems using scattering theory has beed studied before [31]. On top of that, the scattering theory and Landauer-Büttiker formalism has been used to study heat transport in multi terminal normal

conducting structures [32]. As discussed above, it is now worthwhile to employ the scattering matrix approach to study heat transport in superconducting hybrid systems as well.

We describe this formalism for the calculation of heat currents in normal and superconducting junctions in more detail in Chapter 2. Therefore, we set up the scattering matrix description for electron- and hole-like quasiparticle states in superconductors, which are described by Bogoliubov-De Gennes equations.

Finally, in Chapters 3 and 4 we derive an explicit scattering matrix for multi-channel NS and SNS junctions. The resulting transmission probabilities can then be used to calculate the heat current following the Landauer-Büttiker formalism.

1.5 Thesis outline

This thesis comprises our recent study on the statistics of heat conductances in diffusive NS and SNS junctions, as well as some of the required background for these studies.

The thesis is organized as follows. First of all, in Chapter 2, we introduce some basics of the analysis of heat currents and heat conductances in mesoscopic normal conductors using scattering theory within the Landauer-Büttiker formalism. Furthermore, we extend this discussion to quasiparticle excitations in hybrid superconducting junctions described by Bogoliubov-de Gennes equations. Also some general background on heat transport in normal metals is collected in the end of Chapter 2 for comparison. Chapter 3 presents the main results of this thesis. We study phase-dependent heat transport in an SNS junction. We describe the heat conductance in the linear response regime for single-channel conductors as well as for diffusive conductors where an average of the many-channel contributions has to be performed. We furthermore present the weak localization correction to the averaged heat conductance. Finally, the study of heat conductance fluctuations is the key aspect of this chapter. In Chapter 4 a brief overview of heat transport in NS junctions is provided, where we focus on equivalent regimes as the ones studied in Chapter 3. Chapter 5 contains a summary and outlook. We also provide some technical details concerning the derivation of the Landauer-Büttiker heat current formula for superconducting structures, as well as of the full scattering matrices for the multi-channel hybrid setups in the Appendices of this thesis.

2 Methods and Background

Combined structures of superconducting and normal conducting elements form a class of systems in which it is interesting to study transport properties. The main focus of this thesis is to study thermal transport. Specifically, the purpose of this chapter is to provide an introduction about the thermal transport of hybrid superconducting and normal-conducting systems. We discuss methods that we use to study thermal transport in superconducting hybrid structures. The present chapter begins with a discussion of heat transport in bulk metals, which will prove useful when formulating an analogous description for superconducting systems. Next, we introduce superconducting systems in which heat current is carried by quasiparticles living outside the superconducting gap. The behavior of quasiparticle excitations is well explained by the Bogoliubov-de Gennes (BdG) equations. We describe these equations, and then, introduce a scattering matrix theory to study heat currents using Landauer-Buttiker formalism.

2.1 Heat currents and heat conductance in coherent conductors

2.1.1 Heat current

Electrons carry both charge and energy. In a superconductor energy of quasiparticles living above the superconducting gap can be dissipated as heat. The extra energy current with respect to Fermi level is defined as heat current, and it can be expressed in terms of particle and energy currents as follows:

$$J = I^E - \mu I^P. \tag{2.1}$$

The currents I^E and I^P stand for energy and particle currents, respectively, while μ denotes the equilibrium electrochemical potential. The method we use for current calculation is Landauer-Büttiker formula which is based on calculating currents with the help of scattering states. This current can be particle, charge or energy current.

2.1.2 Linear response

In the linear response regime, the temperature difference δT between the left and right leads of a junction is assumed to be small with respect to the equilibrium

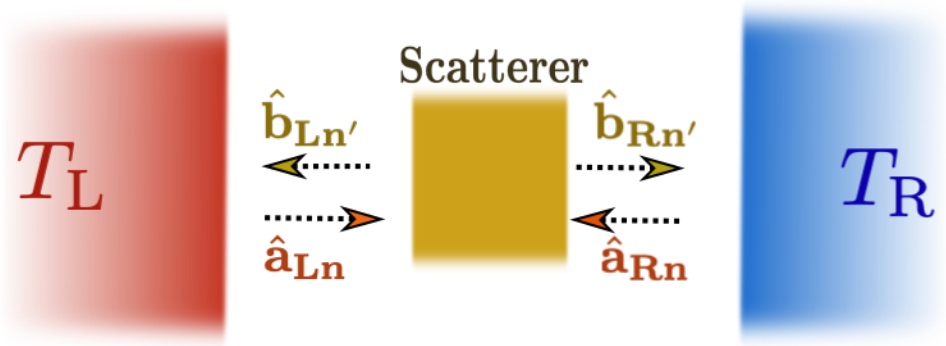

Figure 2.1: *Schematic depiction of a model system involving a scatterer. Incoming and outgoing states in the vicinity of the scatterer are represented by operators $\hat{a}$ and $\hat{b}$.*

temperature T, that is, $T_{\mathrm{L}} = T$ and $T_{\mathrm{R}} = T + \delta T$ with $\delta T \ll T$. Thus, expanding the thermal current in power series of δT in such a regime, we obtain

$$J(T, \delta T) = -\kappa(T)\delta T, \tag{2.2}$$

where $\kappa(T)$ is the temperature dependent heat conductance.

2.1.3 Landauer formula for heat current

A schematic illustration of a metallic scattering region is shown in Fig. (2.1). The scattering region is connected to two reservoirs, which are considered to be in thermal equilibrium. The incoming and outgoing states in the vicinity of the scatterer are indicated in the figure. These states are combinations of plane waves with a real wave number k_n and are also referred to as propagating modes or scattering channels. Particles (electrons or holes) incident on the metallic region are scattered (reflected or transmitted). These particles carry energy as well as charge. Using the Landauer-Büttiker formula [33], we derive the operator for the heat current in a normal conductor

$$\hat{J}_{\alpha,\mathrm{N}}(t,T) = \frac{1}{h}\sum_{n}^{\mathcal{N}}\int_0^\infty dE\, dE'\, e^{i(E-E')t/\hbar} \times \left(\frac{E+E'}{2} - \mu\right)\left[\hat{b}^\dagger_{\alpha n}(E)\hat{b}_{\alpha n}(E') - \hat{a}^\dagger_{\alpha n}(E)\hat{a}_{\alpha n}(E')\right], \tag{2.3}$$

where $\mathcal{N}$ denotes the total number of channels. The operators $\hat{a}_{\alpha n}$ ($\hat{a}^\dagger_{\alpha n}$) represent the amplitudes for the waves coming to the scattering region, whereas $\hat{b}_{\alpha n}$ ($\hat{b}^\dagger_{\alpha n}$) for the waves transmitted or reflected from the scattering region. These operators are related to each other via coefficients which are the elements of a

scattering matrix

$$\hat{b}_{\alpha n} = \sum_{\beta,n'} s_{\alpha n,\beta n'} \hat{a}_{\beta n'}. \tag{2.4}$$

Here, α and β are the lead indices, while the indices n and n' label transport channels. In general, a scattering matrix in a normal metal is block-diagonal and satisfies the symmetry relation

$$S_{\mathrm{N}} = \begin{pmatrix} s_0(\varepsilon) & 0 \\ 0 & s_0(-\varepsilon)^\dagger \end{pmatrix}. \tag{2.5}$$

The two blocks correspond to the scattering matrices for electrons and holes, and they are not coupled in a normal metal. Using polar decomposition [23], the matrix $s_0(\varepsilon)$ can be written in terms of the transmission matrix of the normal region which is a diagonal matrix of dimensions $\mathcal{N}\times\mathcal{N}$ containing the transmission eigenvalues of the normal region, $\mathbf{D} = \mathrm{diag}(D_1, D_2, ..., D_{\mathcal{N}})$,

$$s_0 = \begin{bmatrix} U_1 & \mathbf{0} \\ \mathbf{0} & U_2 \end{bmatrix} \begin{bmatrix} \sqrt{1-\mathbf{D}} & \sqrt{\mathbf{D}} \\ \sqrt{\mathbf{D}} & -\sqrt{1-\mathbf{D}} \end{bmatrix} \begin{bmatrix} V_1 & \mathbf{0} \\ \mathbf{0} & V_2 \end{bmatrix}, \tag{2.6}$$

where U_1, U_2, V_1, V_2 are unitary matrices of dimensions $\mathcal{N}\times\mathcal{N}$. Using the relation for the average of fermionic operators,

$$\langle \hat{a}^\dagger_{\alpha n}(E) \hat{a}_{\beta n'}(E') \rangle = \delta_{\alpha\beta}\delta_{nn'}\delta(E-E') f_\alpha(E), \tag{2.7}$$

we derive the expression for the the average heat current in a normal metal to have the form:

$$J_{\alpha,\mathrm{N}}(T) = \frac{1}{h} \sum_{n=0}^{\mathcal{N}} \int_0^\infty dE\, E D_n \big[f_{\mathrm{L}}(E) - f_{\mathrm{R}}(E) \big]. \tag{2.8}$$

Here, the Fermi function

$$f_\alpha(E) = \frac{1}{1+\exp\big((E-\mu)/(k_{\mathrm{B}}T_\alpha)\big)} \tag{2.9}$$

determines the fermionic particle occupation in the lead α. Note that both leads are kept at the same electrochemical potential μ. The temperature and energy dependence of the Fermi distribution is shown in Fig. (2.2).

2.1.4 Heat conductance

In order to obtain the heat conductance in a normal metal we employ the linear response approximation for small temperature differences δT, see Eq. (2.2). In particular, we approximate the difference of Fermi functions in Eq. (2.8) as follows

$$f_{\mathrm{L}}(E) - f_{\mathrm{R}}(E) \approx -\frac{\partial f(E)}{\partial E} (E-\mu)^2 \frac{\delta T}{T}, \tag{2.10}$$

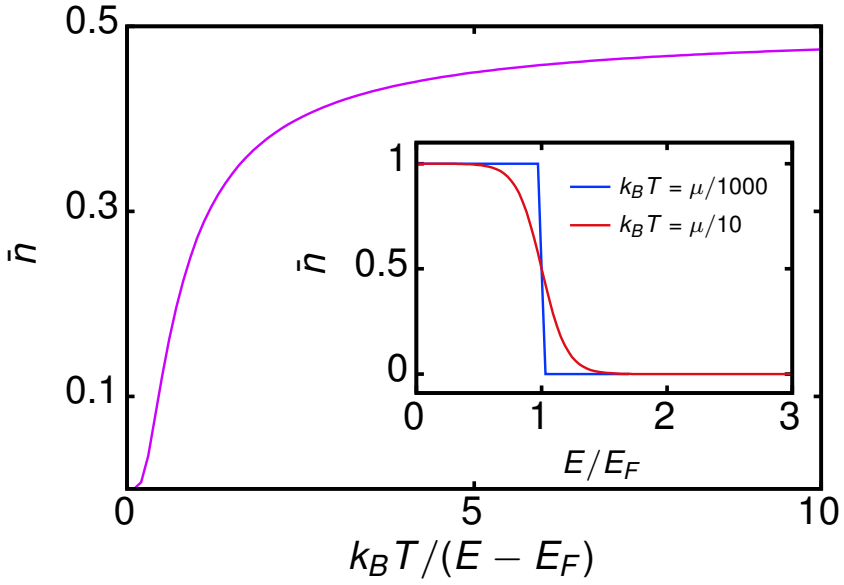

Figure 2.2: *Temperature and energy dependences of the Fermi distribution.*

and consequently, we obtain

$$J_{\mathrm{N}}(T) \approx -\frac{k_B^2 T}{h} \sum_{n=0}^{\mathcal{N}} D_n \int_0^\infty dE \left(\frac{E-\mu}{k_B T}\right)^2 \frac{\partial f}{\partial E} \cdot \delta T. \tag{2.11}$$

We considered the transmission eigenvalues D_n to be energy independent. Such an assumption allows for calculating analytically the energy integral in the equation above, yielding

$$\int_0^\infty dE \left(\frac{E-\mu}{k_B T}\right)^2 \frac{\partial f}{\partial E} = -\frac{\pi^2}{3}. \tag{2.12}$$

As a result, the heat current in the linear response regime takes the form

$$J_{\mathrm{N}}(T) = \frac{\pi^2 k_B T}{3h} \sum_{n=0}^{\mathcal{N}} D_n \cdot \delta T \equiv \kappa_{\mathrm{N}}(T) \cdot \delta T. \tag{2.13}$$

The heat conductance of a normal metal $\kappa_{\mathrm{N}}(E)$ corresponds simply to the heat conductance quantum, defined as $\kappa_0 = \pi^2 k_B T/(3h)$, multiplied by the sum over transmission eigenvalues.

2.2 Heat currents and heat conductance in superconductors

Now, after reviewing the scattering formalism for heat transport in a normal metal, we introduce the scattering formalism for a superconductor and we show how the scattering problem formulated in the previous section changes. For this

reason, we recall the BdG equation which explains the behavior of superconducting states.

2.2.1 Bogoliubov-De Gennes equation

The scattering states in superconductor are eigenfunctions of the BdG equation that has the form of two Schrödinger equations for electron and hole wave functions coupled by the superconducting energy gap.

$$i\hbar\frac{\partial f}{\partial t} = \left[-\frac{\hbar^2\nabla^2}{2m} - \mu(x) + V(x)\right] f(x,t) + \Delta(x)g(x,t), \tag{2.14a}$$

$$i\hbar\frac{\partial g}{\partial t} = -\left[-\frac{\hbar^2\nabla^2}{2m} - \mu(x) + V(x)\right] g(x,t) + \Delta(x)f(x,t). \tag{2.14b}$$

Here $\Delta(x)$ is the space dependent energy gap and $\mu(x)$ is the chemical potential. In a normal metal [that is, for $\Delta(x) = 0$], Eqs. (2.14) are two independent Schrödinger equations for electrons and holes. On the contrary, in a superconductor we have $\Delta(x) \neq 0$, and the electron and hole wave functions are coupled. We now assume that $\mu(x), \Delta(x)$ and $V(x)$ are all constant. As a result, the solutions for Eqs. (2.14) are plane waves $f = ue^{ikx-iEt/\hbar}$ and $g = ve^{ikx-iEt/\hbar}$. The amplitude $|v|^2$ represents the probability that a pair of states $(\mathbf{k}, -\mathbf{k})$ is occupied, whereas $|u|^2$ is the probability that such a pair of states is unoccupied, which also implies $|u|^2 + |v|^2 = 1$. In the absence of a external field $V = 0$, substituting f and g into (2.14) gives:

$$Eu = \left(\frac{\hbar^2k^2}{2m} - \mu\right) u + \Delta v, \tag{2.15a}$$

$$Ev = -\left(\frac{\hbar^2k^2}{2m} - \mu\right) v + \Delta u. \tag{2.15b}$$

Now, we want to obtain the dispersion relation for a superconductor. To do this, we need to calculate u or v by solving the set of equations (2.15). Eventually, this procedure allows for finding the Bogoliubov spectrum (dispersion relation)

$$E^2 = \left(\frac{\hbar^2k^2}{2m} - \mu\right)^2 + \Delta^2, \tag{2.16}$$

which is also illustrated in Fig. (2.3). Solving the equation above for wave vector, we get

$$\hbar k^{\pm} = \sqrt{2m\left(\mu \pm \sqrt{E^2 - \Delta^2}\right)}. \tag{2.17}$$

The two momenta k^+ and k^- correspond to particle- (electron-) and hole-like excitations, respectively. Knowing that $|u|^2 + |v|^2 = 1$, we have the energy dependences of u and v

$$|u|^2 = \frac{1}{2}\left(1 \pm \frac{(E^2 - \Delta^2)^{1/2}}{E}\right) = 1 - |v|^2. \tag{2.18}$$

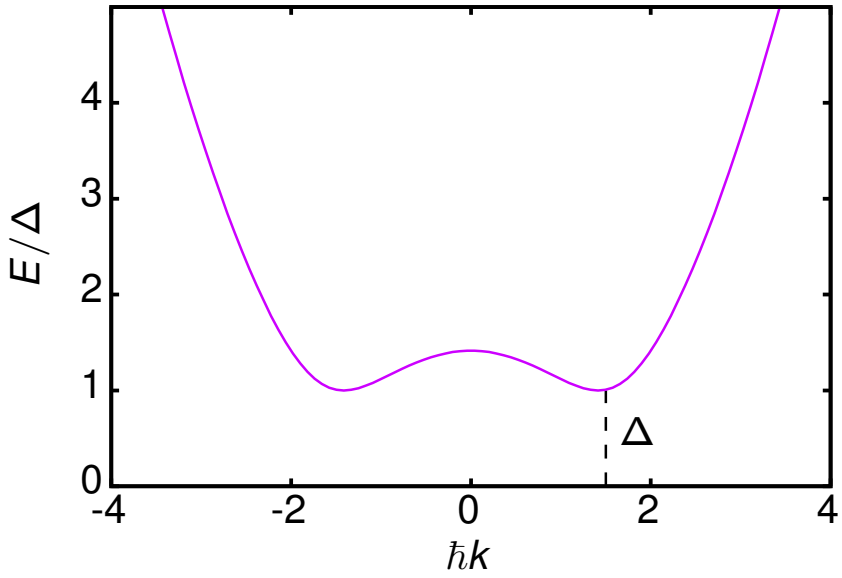

Figure 2.3: *Dispersion relation for a superconductor, see Eq. (2.16), showing the energy gap of a superconductor.*

The Bogoliubov spectrum illustrated in Fig. (2.3) corresponds to the spectrum of quasiparticles in the excited band, out of superconducting energy gap. In order to represent the energy levels in a superconductor more clearly let us consider the following model. A superconductor has an energy gap of Δ between two energy bands. As shown in Fig. (2.4), at zero temperature, the lower band is full of electrons and the higher band is empty. By increasing temperature, some of the electrons move from the lower to the upper band. These excited electrons are called quasielectrons (or quasiparticles). They act approximately like normal conduction electrons in the sense that they move at Fermi velocity v_F. These electrons lose the energy Δ by falling from the bottom of the upper band to the top of the lower band. As was explained earlier, the probability of the state $\mathbf{k}$ to be empty and ready to receive an incoming electron is $|u|^2$, see Eq. (2.18) [34]. The Fermi energy level is considered at the center of the gap. This picture is called the semiconductor representation model of a superconductor [35].

2.2.2 Scattering theory for heat currents in a superconductor

Now, we develop the Landauer formula for heat currents in a superconducting region. In appendix (A) we derive the formula for the heat-current operator in a superconductor. Setting the electrochemical potential $\mu = 0$, the result takes the form

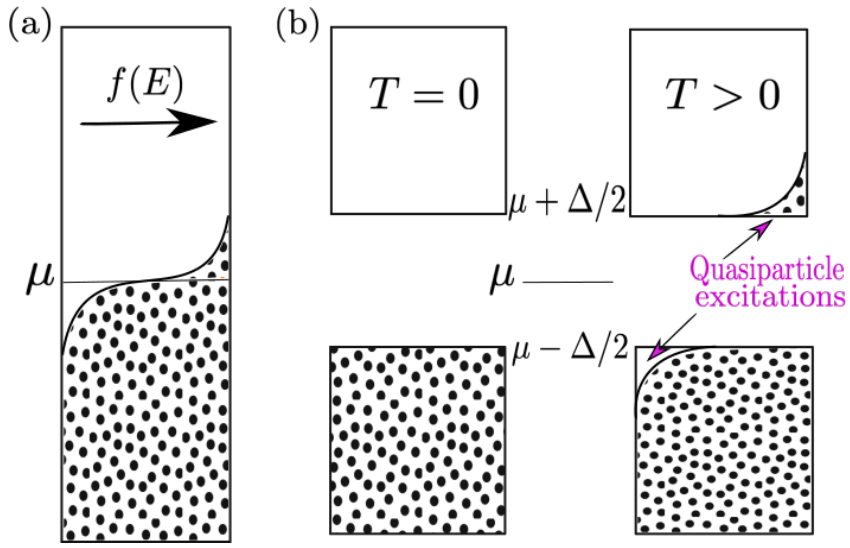

Figure 2.4: *(a) Schematic diagram of energy levels for a normal metal with Fermi distribution shown at finite temperature. The Fermi energy level is denoted by μ. (b) Semiconductor picture of energy levels of a superconductor at $T = 0$ and $T > 0$. The gap of superconductor is Δ. The dotted areas indicate occupied electronic states.*

$$\hat{J}(t,T)_{\alpha,\mathrm{S}} = \frac{1}{h}\sum_{n}^{\mathcal{N}}\sum_{i=e,h}\int_{\Delta}^{\infty} dE\, dE'\, e^{i(E-E')t/\hbar} \times \left(\frac{E+E'}{2}\right)\left[\hat{\mathrm{b}}^{\dagger}_{i,n}(E)\hat{\mathrm{b}}_{i,n}(E') - \hat{\mathrm{a}}^{\dagger}_{i,n}(E)\hat{\mathrm{a}}_{i,n}(E')\right]. \quad (2.19)$$

In the expression above, there are two parts for electron- ($i = e$) and hole-like ($i = h$) quasiparticle contributions to the heat current with a sum over $\mathcal{N}$ transport eigenchannels in a superconducting lead. The gap Δ in the lower limit of integration should be understood as the maximum gap in the case we have different superconducting leads with unequal gap functions. Here, the operators $\hat{a}^{(\dagger)}_{i,n}$ ($\hat{a}_{i,n}$) and $\hat{b}^{(\dagger)}_{i,n}$ ($\hat{b}_{i,n}$) represent incoming and outgoing states to the superconductor's junction and in this case they indicate Bogoliubov operators. As mentioned before, the incoming and outgoing states are related to each other by a scattering matrix specific to the junction under consideration. The BdG equation is used together with wave function matching in appendices (B and C) to construct the scattering matrix of a superconducting hybrid junction. Calculating the average of the heat-current operator in Eq. (2.19), analogously as in the case of normal leads, we obtain the average heat current that depends on the transmission probabilities of electrons and holes,

$$J_{\alpha,\mathrm{S}}(T) = \frac{1}{h}\sum_{n=0}^{\mathcal{N}}\int_{\Delta}^{\infty} dE\, E\left[\mathcal{D}^{e}_{n} + \mathcal{D}^{h}_{n}\right]\left[f_{\mathrm{L}}(E) - f_{\mathrm{R}}(E)\right], \quad (2.20)$$

where Fermi functions $f_\alpha(E)$, Eq. (2.9), determine the quasiparticle occupation in superconducting contacts, $\alpha \equiv$ L,R. The transmission probability of channel n consists of electron-like and hole-like quasiparticles contributions that are equal due to particle hole symmetry ($\mathcal{D}_n^e = \mathcal{D}_n^h$). The transmission probability $\mathcal{D}_n^e$ is a sum of transmission probabilities of electron-like and whole-like quasiparticles to the electron-like channels, $\mathcal{D}_n^e = \mathcal{D}_n^{ee} + \mathcal{D}_n^{eh}$. These transmission probabilities are calculated using scattering matrices for NS and different regimes of SNS junctions in the next chapters.

2.2.3 Heat conductance

In order to derive the linear response heat conductance in a superconductor we consider the difference of Fermi functions at small temperature differences of two leads to be

$$f_{\mathrm{L}}(E) - f_{\mathrm{R}}(E) = \frac{E}{4k_B T^2 \cosh^2\Big(E/(2k_B T)\Big)} \cdot \delta T. \tag{2.21}$$

Substituting the equation above into Eq. (2.20) and employing the linear response relation (2.2), we obtain the formula for the heat conductance in a superconducting lead

$$\kappa_{\mathrm{S}}(T) = \frac{1}{2h} \sum_{n=0}^{\mathcal{N}} \frac{1}{k_B T^2} \int_\Delta^\infty dE \, \frac{E^2}{\cosh^2\Big(E/(2k_B T)\Big)} \mathcal{D}_n^e. \tag{2.22}$$

Here, we also made use of the particle-hole symmetry which basically means that the transmission probabilities of electron-like ($\mathcal{D}_n^e$) and hole-like ($\mathcal{D}_n^h$) quasiparticles are equal.

2.3 Thermal conductivity of the normal state

Befor we analyze heat transport in superconducting structures for specific junctions, it is intuitive to review the mechanisms of thermal conductivity in a normal metal. In such a case, carriers of thermal energy are electrons and phonons which have two independent channels. Total thermal conductivity can be written as a sum of electronic (κ_e) and phononic (κ_e) contributions,

$$\kappa_{\mathrm{N}} = \kappa_e + \kappa_{ph}. \tag{2.23}$$

Moreover, the electronic conductivity has electron-lattice contribution $\kappa_{e-\mathrm{L}}$ and the impurity term $\kappa_{e-\mathrm{I}}$, whereas the phonon conductivity contains phonon-electron κ_{ph-e} and impurity $\kappa_{ph-\mathrm{I}}$ contributions. Each pair of conductivities involving the same carriers of heat act in series. Considering pure metals, the electron-lattice

contribution of electronic conductivity will be important. From solid state physics we know [35]

$$\kappa_{e-\mathrm{L}} = \frac{1}{3} v_F l C_e, \tag{2.24}$$

where $l = v_F \tau$ is the mean free path and $C_e = \gamma T$ stands for the conduction-electron contribution to the specific heat. Here, $\gamma = \frac{\pi^2}{3} D(E_F) k_B^2$ is the Sommerfeld constant with the density of state defined as $D(E_F) = (m^* k_F)/(\hbar^2 \pi^2)$ and m^* representing the effective mass. Temperature dependence of relaxation time is

$$\tau = \begin{cases} T^{-3}, & \text{for } T \ll \Theta_D, \\ T^{-1}, & \text{for } T \gg \Theta_D, \end{cases} \tag{2.25}$$

where Θ_D is the Debye temperature. Combining Eqs. (2.24)-(2.25), we can explicitly write the temperature dependence of the lattice contribution to the electronic thermal conductivity

$$\kappa_{e-\mathrm{L}} = \begin{cases} \dfrac{\text{const}}{T^2}, & \text{for } T \ll \Theta_D, \\ \text{const}, & \text{for } T \gg \Theta_D. \end{cases} \tag{2.26}$$

In order to obtain the temperature dependence of the impurity contribution to the electronic thermal conductivity we consider the Wiedemann-Franz law $\kappa_{\mathrm{th}}/\sigma = (3/2)(k_B/e)^2 T$, knowing that the electrical conductivity at low temperatures is temperature independent, $\sigma(T) = \sigma_0$. As a result, $\kappa_{e-\mathrm{I}} = \text{const} \cdot T$ at $T \to 0$. We also note that in pure metals, the electronic contribution to the thermal conductivity tends to dominate at all temperatures. Finally, comparing Eq. (2.26) with the heat conductance we obtained for a normal metal in linear response regime Eq. (2.24). Thus, we conclude that the Drude's model is applicable for temperatures larger that the Debye temperature.

3 Heat Conductance and Heat Conductance Fluctuations in SNS Junctions

In the previous chapter, we presented the scattering theory for heat currents in normal and superconducting devices. In this chapter, we use this formalism to study thermal transport in an SNS junction with a disordered normal region. In order to use scattering theory to study heat currents we first construct the scattering matrix of the SNS junction. Following Ref. [36], we express the scattering matrix of the SNS junction in terms of the transmission eigenvalues of the disordered normal region. The obtained transmission probabilities are then used to calculate the heat current and the linear response heat conductance.

With this, in a first step, we are able to reproduce previous results for SIS junctions (in the absence of a diffusive junction), as experimentally proven in Ref. [9]. We then come to the main focus of this chapter and study the statistical contribution of many transport channels to the heat conductance using the DMPK formula, based on random matrix theory (RMT) [23]. This formula suggests a bimodal distribution of transmission eigenvalues of the disordered normal region, dependent on the length of the junction.

In the channel average of the heat conductance, obtained from this, we find that the phase dependence is fully suppressed. The properties of the superconductor barely enter via the magnitude of the gap compared to the temperature, which determines the occupation of quasiparticles. We then calculate the weak localization correction to this average, which interestingly maintains the phase dependent behavior. Finally, we address the variance of the heat conductance in Josephson junctions (SNS). Conductance fluctuations of the charge current in normal diffusive conductors have been of interest since several decades; their most important feature is their universal behavior [24–26]. The heat conductance fluctuations in an SNS junction, have however not been addressed before. Here, we show that they are similarly universal, but have an additional temperature dependence, induced by the phase difference between the superconductors.

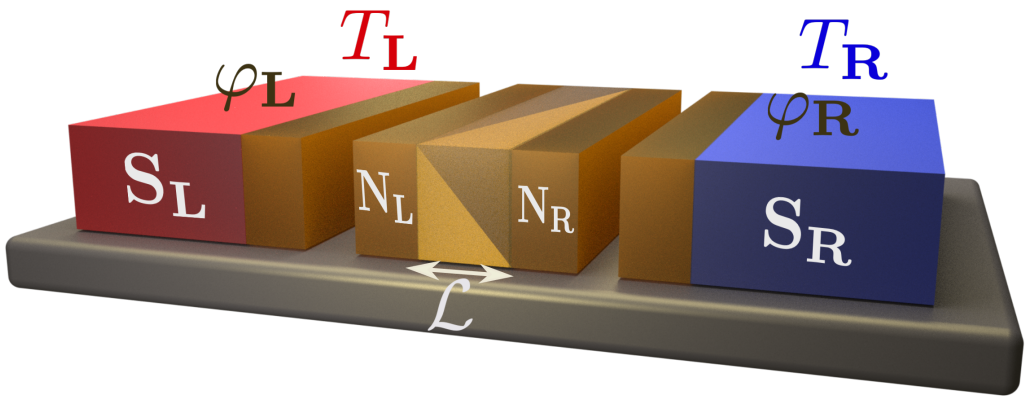

Figure 3.1: *Sketch of an SNS junction consisting of two superconducting leads characterized by different temperatures and phases. Assuming a generic barrier in the normal region, we construct the scattering matrix of the whole SNS junction in terms of the normal scattering matrix of the barrier.*

3.1 Superconductor-normal metal-superconductor (SNS) junction

In this section we explain the construction of the scattering matrix of an SNS junction. The model we consider is shown schematically in Fig. 3.1. It consists of a normal region containing a generic barrier or a disordered part between two superconducting regions S_L and S_R. Incoming and outgoing states in normal and superconducting regions are indicated in figure (3.2)

In Appendix C the scattering matrix of an SNS junction is derived in terms of the normal region scattering matrix. In order to obtain a well defined scattering matrix we assume two ideal normal leads at the left and right of the disordered region, N_L and N_R. We assume that the disorder is only contained in the normal region. This separation of scatterings in the disordered normal region and the normal-superconductor interface is illustrated in Fig. (3.1). It allows us to simplify the scattering matrix of a SNS junction by relating it directly to the normal scattering matrix. This model is valid in superconductor clean limit where the electron mean free path l is large compared to the superconducting coherence length ξ ($l \gg \xi$). Therefore the SNS junction we consider will be divided into three junctions, NS, NN and SN junctions. By writing down the scattering matrix of each junction separately and combining the three matrices, we have the scattering matrix of SNS junction. For a Josephson junction shown in figure (3.2) containing

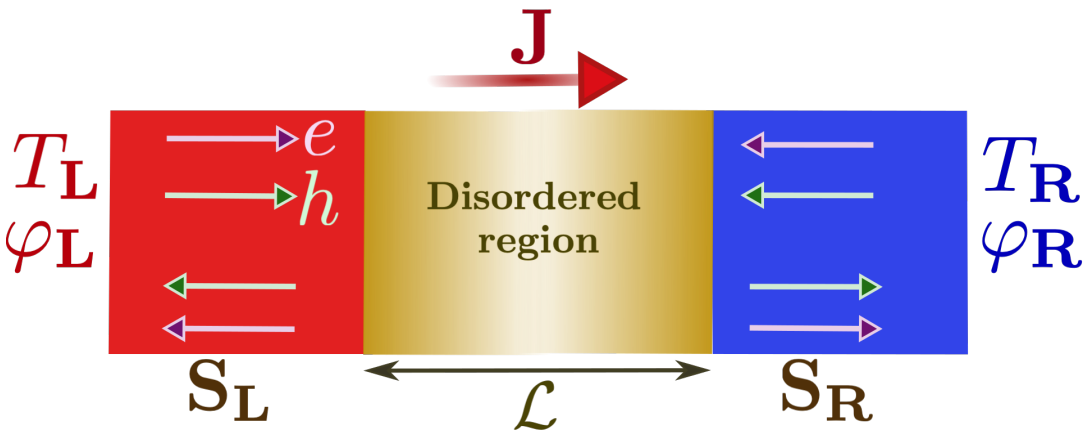

Figure 3.2: *Sketch of an SNS junction across which a temperature as well as a phase difference occurs. The normal part of the junction has length $\mathcal{L}$ and supports $\mathcal{N}$ scattering channels. We consider the normal region to be disordered.*

a disordered normal region the scattering matrix has the following structure

$$S_{\mathrm{SNS}} = U^{-1}(\mathbf{1} - M)^{-1}(\mathbf{1} - M^{\dagger})S_{\mathrm{N}}U. \tag{3.1}$$

This matrix is written in terms of the normal scattering matrix, S_{N}. Thus having normal scattering matrix, we can study the properties of the whole SNS junction. In derivation of this scattering matrix we used the trick from Ref. [37] that is, we considered a generic barrier in the middle of the normal part. The matrices in the formula (3.1) are defined as follows

$$U \equiv \begin{bmatrix} \nu & 0 \\ 0 & \nu^* \end{bmatrix}, \quad \nu \equiv \begin{bmatrix} \frac{e^{i\varphi_{\mathrm{L}}/2}}{\cos\alpha_{\mathrm{L}}} & \mathbf{0} \\ \mathbf{0} & \frac{e^{i\varphi_{\mathrm{R}}/2}}{\cos\alpha_{\mathrm{R}}} \end{bmatrix},$$

The matrix U is a unitary matrix and contains the terms which vanish in the process of calculating transmission probabilities using the scattering matrix. The phases of matrix U disappear due to the multiplication of the unitary matrix by its inverse. Therefore this matrix U does not have any effect on the final transmissions that are related to transport properties. Calculating the transmission probabilities through S_{SNS}, the phase dependence of transmission amplitudes is due to Andreev reflection which enters the scattering matrix via r_A and is defined as follows

$$M \equiv S_{\mathrm{N}} \begin{bmatrix} 0 & r_A \\ r_A^* & 0 \end{bmatrix}, \quad r_A \equiv \begin{bmatrix} \sin\alpha_{\mathrm{L}} e^{i\varphi_{\mathrm{L}}} & \mathbf{0} \\ \mathbf{0} & \sin\alpha_{\mathrm{R}} e^{i\varphi_{\mathrm{R}}} \end{bmatrix}.$$

Here r_A contains the terms which are the results of Andreev scattering with defined as $\sin\alpha_{\mathrm{L(R)}} = v_{\mathrm{L(R)}}/u_{\mathrm{L(R)}}$, $u_{\mathrm{L(R)}} = \sqrt{\Delta_{\mathrm{L(R)}}/2E}e^{\mathrm{arcosh}(E/\Delta_{\mathrm{L(R)}})/2}$ and $v_{\mathrm{L(R)}} =$

$\sqrt{\Delta_{\mathrm{L(R)}}/2E}e^{-\mathrm{arcosh}(E/\Delta_{\mathrm{L(R)}})/2}$. The temperature dependent gaps of the left and right superconducting leads are $\Delta_{\mathrm{L(R)}}$.
The normal scattering matrix contains two separate blocks for electrons and holes which are not coupled

$$S_{\mathrm{N}} = \begin{bmatrix} s_0(\varepsilon) & 0 \\ 0 & s_0(-\varepsilon)^{\dagger} \end{bmatrix}. \tag{3.2}$$

Using polar decomposition [23], the matrix $s_0(\varepsilon)$ can be written in terms of the transmission eigenvalues of the disordered normal region which is an $\mathcal{N} \times \mathcal{N}$ diagonal matrix of normal transmission eigenvalues ($\mathbf{D}$). This matrix brings the effect of many transport channels supported by the disordered normal region to SNS scattering matrix.

$$s_0 = \begin{bmatrix} U_1 & \mathbf{0} \\ \mathbf{0} & U_2 \end{bmatrix} \begin{bmatrix} \sqrt{1-\mathbf{D}} & \sqrt{\mathbf{D}} \\ \sqrt{\mathbf{D}} & -\sqrt{1-\mathbf{D}} \end{bmatrix} \begin{bmatrix} V_1 & \mathbf{0} \\ \mathbf{0} & V_2 \end{bmatrix}. \tag{3.3}$$

Here the matrices U_1, U_2, V_1, V_2 are four $N \times N$ unitary matrices.

Transport properties are related to transmission probabilities through junctions. Therefore from the scattering matrix (3.1) we obtain the transmission probability through the SNS junction in order to apply it into heat transport quantities. The full transmission probability is a sum over transmissions of $\mathcal{N}$ transport channels, D_n. We are interested in this summation since we want to study the case where there are many channels contributing to transport, as it is in disordered conductors. The transmission probabilities into electron-like quasiparticle channel is the sum of transmissions from electron- and hole-like quasiparticels, $\mathcal{D}_n^{ee} + \mathcal{D}_n^{eh}$, and is given by

$$\mathcal{D}_n^{e}(E) = 2D_n\xi_{\mathrm{L}}\xi_{\mathrm{R}} \frac{D_n\xi_{\mathrm{L}}\xi_{\mathrm{R}} + (2-D_n)(E^2 - \Delta_{\mathrm{L}}\Delta_{\mathrm{R}}\cos\varphi)}{((2-D_n)\xi_{\mathrm{L}}\xi_{\mathrm{R}} + D_n(E^2 - \Delta_{\mathrm{L}}\Delta_{\mathrm{R}}\cos\varphi))^2}, \tag{3.4}$$

where $\xi_{\mathrm{L(R)}} = \sqrt{E^2 - \Delta_{\mathrm{L(R)}}^2}$ is the quasiparticle energy in the contact L(R). The phase difference between left and right superconductors is $\varphi = \varphi_{\mathrm{L}} - \varphi_{\mathrm{R}}$. This result is important since it is the general transmission which is valid for the case of unequal superconducting gaps $\Delta_{\mathrm{L}} \neq \Delta_{\mathrm{R}}$. Another important aspect of this transmission is that it supports different limits of D_n including arbitrary strong normal transmissions. From this general result we can reproduce all other limiting cases as follows.

Now, we look at different limits of this transmission probability. For small D_n, by expanding the transmission amplitude in Eq. (3.4) up to first order in D_n, we obtain the transmission probability in tunneling regime with which we reproduce the results of heat conductance obtained by Maki-Griffin [2]

$$\mathcal{D}_n^{e}(E) = D_n \frac{E^2 - \Delta_{\mathrm{L}}\Delta_{\mathrm{R}}\cos\varphi}{\xi_{\mathrm{L}}\xi_{\mathrm{R}}}. \tag{3.5}$$

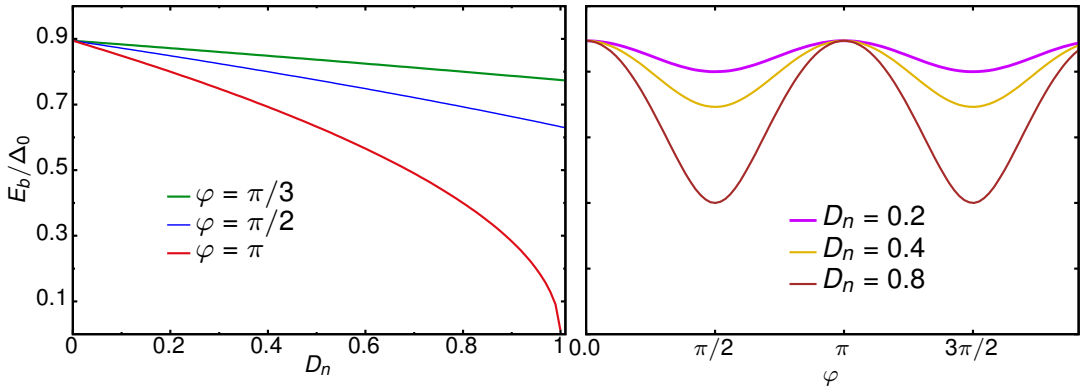

Figure 3.3: *Phase and transmission dependence of the Andreev bound state energy. The temperature is $T/T_{crit} = 0.2$ and Δ_0 is the superconducting energy gap at zero temperature.*

This result is only valid for small D_n.

Another limit of interest is the opposite case of small transmissions which corresponds to a fully transparent junction when $D_n = 1$. In this case the only transmission in the whole junction is from electron-like to electron-like quasiparticles and $\mathcal{D}^{eh} = 0$. The transmission probability in this case is given by

$$\mathcal{D}_n(E) = \mathcal{D}^{ee}(E) = \frac{2\xi_{\mathrm{L}}\xi_{\mathrm{R}}}{E^2 + \xi_{\mathrm{L}}\xi_{\mathrm{R}} - \Delta_{\mathrm{L}}\Delta_{\mathrm{R}}\cos\varphi}. \tag{3.6}$$

Finally, in the linear response regime which we consider to calculate the conductance, the temperature difference of the two superconducting leads is small. Therefore the temperature dependence of the energy gap of the two leads will be equal. This requires finding the transmission amplitude for equal superconducting gaps. Therefore considering equal superconducting leads with equal gaps and substituting $\Delta_{\mathrm{L}} = \Delta_{\mathrm{R}}$ in the expression (3.4) we obtain

$$\mathcal{D}_n^{ee} = D_n \frac{\xi^2(E^2 - \Delta_0^2\cos^2(\varphi/2))}{(E^2 - E_b^2)^2}, \qquad \mathcal{D}_n^{eh} = D_n(1-D_n)\frac{\xi^2\Delta_0^2\sin^2(\varphi/2)}{(E^2 - E_b^2)^2}, \tag{3.7}$$

and therefore

$$\mathcal{D}_n^{e} = \frac{(E^2 - \Delta^2)}{(E^2 - E_b^2)}[D_n(E^2 - \Delta^2\cos\varphi) - D_n^2\Delta^2\sin^2(\varphi/2)]. \tag{3.8}$$

Here, $E_b = \Delta\sqrt{1 - D_n\sin^2(\varphi/2)}$ is the Andreev bound state energy. Multiple Andreev reflections lead to formation of sub-gap states which are called Andreev bound states, with energies below the superconducting gap. These states influence the transmissions above the gap. In Fig. (3.3) dependence of this energy on the transmission D_n and phase is shown at the temperature $T/T_{\mathrm{crit}} = 0.2$. It is visible from the plots that the bound state energy has significant temperature and phase

dependence, and this influences the heat conductance. This influence is missing in the weak coupling regime where D_n is small.

In the case when there is no phase difference between superconducting leads, $\varphi = 0$, as well as the case of zero gap function, $\Delta = 0$, we obtain the transmission (3.8) which is equal to the normal transmission, $\mathcal{D}_n^e = D_n$. This behavior is the same as for similar limits of conductance for which we obtain the results in the next sections.

3.2 Heat conductance and averaging

We have derived the formula for heat conductance in a superconducting junction in Section (2.2.3). The heat conductance calculated in the linear response regime is

$$\kappa_{\mathrm{SNS}} = \frac{1}{2h}\sum_{n=0}^{\mathcal{N}} \frac{1}{k_{\mathrm{B}}T^2}\int_{|\Delta|}^{\infty} dE \frac{E^2}{\cosh^2(\frac{E}{2k_{\mathrm{B}}T})}\,\mathcal{D}_n^e(E)|_{\delta T=0} \tag{3.9}$$

where $\mathcal{D}_n^e(E)$ is the full transmission in Eq. (3.4).

Assuming the equal temperature dependent superconducting gap functions ($\Delta_{\mathrm{L}} = \Delta_{\mathrm{R}}$) and substituting the transmission probability given in Eq. (3.8) in the formula for heat conductance gives us the heat conductance of an SNS junction with equal gaps for superconducting leads

$$\begin{aligned}\kappa_{\mathrm{SNS}}(T) = \frac{1}{2h}\sum_{n=0}^{\mathcal{N}} \frac{1}{k_B T^2}\int_{\Delta}^{\infty} dE \frac{E^2}{\cosh^2(E/2k_BT)} \\ \times \frac{(E^2-\Delta^2)}{(E^2-E_b^2)}[D_n(E^2-\Delta^2\cos\varphi) - D_n^2\Delta^2\sin^2(\varphi/2)].\end{aligned} \tag{3.10}$$

The transmission probability of the disordered normal region, D_n takes the values between 0 and 1. For superconducting contacts with $\Delta_{0,\mathrm{L}} = \Delta_{0,\mathrm{R}} = \Delta_0$ (made of the same material), we recover previously obtained result in the single- [22] and multi-channel regime [7, 8]. Note that results obtained in the tunneling limit [2, 38] are only valid for heat currents at relatively large temperature gradients and the heat *conductance* is hence not straightforwardly obtained from this. With Eqs. (3.4) and (3.10), we confirm an important result of Ref. [8], namely that the heat conductance κ_{SNS} shows a phase- and transmission-dependent increase with respect to the value of a fully normal-conducting device $\kappa_{\mathrm{N}} = \kappa_0 \sum_{n=0}^{\mathcal{N}} D_n$. Here, $\kappa_0 = \frac{\pi^2 k_{\mathrm{B}}^2}{3h}T$ is the (temperature-dependent) heat conductance quantum [39], recently measured in electronic systems [40].

The heat conductance behavior for a single channel is shown in Fig. (3.4). When the temperature reaches the critical point of the superconductor, the heat conductance is equal to the normal heat conductance as shown in the figure. For some transmissions the heat conductance is larger than the normal case at

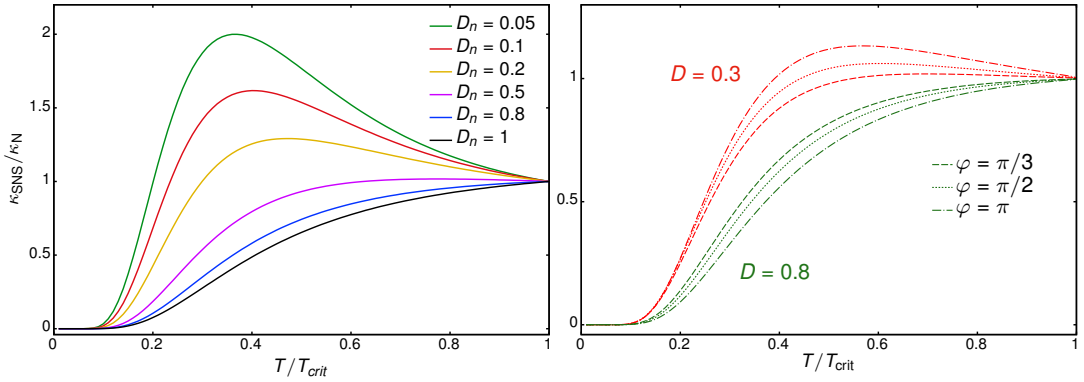

Figure 3.4: *Temperature dependence of single channel heat conductance of SNS junction (Left) Equal superconducting gaps at different transmissions of disordered normal region. The phase difference of the two superconductors here is $\varphi = \pi$. (Right) Different superconducting gaps at different phases and transmissions. Heat conductance increases to values larger than these for normal heat conductance for smaller transmissions.*

temperatures smaller than T_{crit}. We set the phase difference of the two superconductors to $\varphi = \pi$ which has the most effect comparing to other phase differences. These results agree well with previous studies [8]. The phase dependence of single channel heat conductance for different transmissions is shown in Fig. (3.5).

Now, we come to the case where the conductance is affected by large number of channels. We consider a disordered region to exist in the normal barrier in the model we study. This barrier supports $\mathcal{N}$ transport channels. In order to take into account the effect of many channels in the heat conductance we take average of all channels. To compute this average we need to know how the transmission eigenvalues are distributed. The distribution function of transmission eigenchannels of a diffusive conductor is computed by Dorokhov [41], Mello and Pichard [42]. They consider a wire with length $\mathcal{L}$ which has random impurities. The scattering of such a wire is random. By considering an ensemble of RMT (Random Matrix Theory) for transmission probabilities, the distribution of transmission probabilities is obtained and it depends on the length of the wire (or junction in our model)

$$\rho(D_n) = \frac{l}{2\mathcal{L}D_n\sqrt{1-D_n}}. \tag{3.11}$$

In order to calculate the average of heat conductance we multiply it by the DMPK equation and integrate over all transmissions

$$\langle \kappa_{\text{SNS}} \rangle = \int_0^1 dD_n \rho(D_n) \kappa_{\text{SNS}}. \tag{3.12}$$

This ensemble average of heat conductance is of the first order in $l/\mathcal{L}$ which comes from the length dependence of Dorokhov distribution. Using a trick developed in

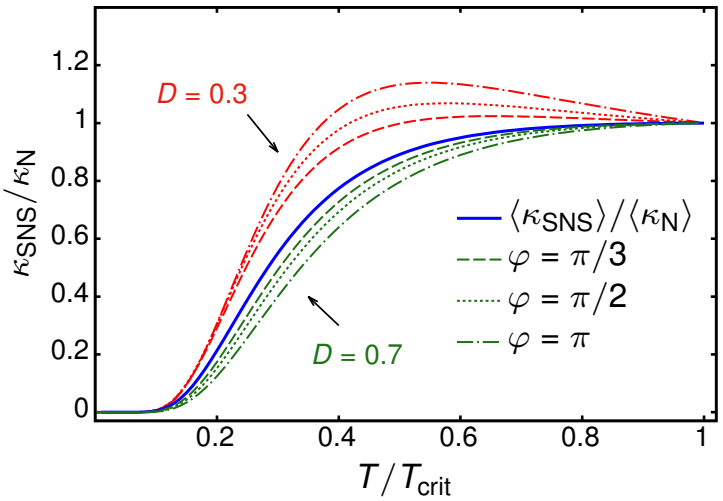

Figure 3.5: *Temperature modulation of average heat conductance* $\langle\kappa_{SNS}\rangle$ *scaled to single-channel heat conductance* κ_{SNS}/κ_N *for different values of* φ *and* $D_n = 0.3$ *and* 0.7. *These results are obtained for the equal gaps of the left and right superconductors. Results for average heat conductance* $\langle\kappa_{SNS}\rangle/\langle\kappa_N\rangle$ *are phase-independent and exactly coincide with the transmission-independent single-channel results* κ_{SNS}/κ_N *at* $Ï† = 0$.

chapter 2 of Ref. [33] based on a parametrization of the transmission eigenvalues D_n, this integral can be solved analytically and we find

$$\frac{\langle\kappa_{\rm SNS}\rangle}{\langle\kappa_{\rm N}\rangle} = 2 - \frac{6}{\pi^2}\left[\left(\frac{|\Delta|}{k_{\rm B}T}\right)^2 (1 - f(|\Delta|)) + 2\frac{|\Delta|}{k_{\rm B}T}\ln f(|\Delta|) - 2{\rm Li}_2\left(-e^{|\Delta|/k_{\rm B}T}\right)\right], \tag{3.13}$$

with the dilogarithmic function Li_2. This key result shows that $\langle\kappa_{\rm SNS}\rangle$ in a disordered SNS junction is *fully phase-independent*. The average heat conductance $\langle\kappa_{\rm SNS}\rangle/\langle\kappa_{\rm N}\rangle$ equals the single-channel result at vanishing phase difference $\delta\varphi = 0$. In Fig. (3.5) the average of SNS heat conductance normalized to the normal heat conductance average is shown. As one can see, although the single channel heat conductance is phase dependent, this dependence disappears by taking the average (The blue plot in the figure shows the average of the single channel heat conductance for zero phase difference which are equal). This is how DMPK distribution influences averaging by considering different weights for transmission eigenvalues. Both single channel and average of heat conductances also show a suppression in very small temperatures.

Considering the Lorentzian shape for transmission eigenvalues, $D_n = 1/(1 + (\chi/\omega)^2)$, and computing the average of transmission probability of the SNS junction, Eq. (3.8), using the DMPK distribution, we obtain

$$\int dD_n \mathcal{D}^e(D_n)\rho(D_n) = \int d\chi D_n^{1/2}\mathcal{D}^e(\chi) = \omega. \tag{3.14}$$

Therefore we see a witness which shows the phase dependence disappears by averaging over transmission eigenvalues which are distributed by the DMPK distribution. We conclude that the transmissions D_n are not distributed uniformly according to Dorokhov distribution and they are either exponentially small or of the order of unity.

3.3 Weak localization

A theory of localization in multimode wires has been introduced by Dorokhov [43] and Mello, Pereyra, and Kumar [44]. Due to enhanced backscattering of carriers [45] and the resulting interference between time-reversed paths, the average quantum conductance is smaller than the classical one. This has been verified by a numerical experiment for a conductor containing 30 transport channls [46]. This is one of the very important phase-coherent mesoscopic effects. This effect is known as the weak localization and occurs on length scales $\mathcal{L} \ll \mathcal{N}l$, where the length of the conductor or the junction length is much smaller than the localization length. Here l is the mean free path and $\mathcal{N}l$ the localization length. This regime corresponds to the short junction limit. In a long junction, where the junction length is comparable to the localization length, electrons are localized. This is the strong localization regime. For a metallic conductor it is not very probable to enter the strong localization regime, however, the weak localization has been observed in metallic wires at very low temperatures [47].

The resulting correction to the average of the heat conductance can be obtained considering the corresponding correction to the distribution of transmission eigenvalues $\delta\rho$. Using the parametrization $D_n = \frac{1}{\cosh^2 x}$ for the transmission eigenvalues of the normal region, one can write $\delta\rho$ for time-reversed and spin-rotation symmetric systems (as the one considered here) as [48].

$$\delta\rho(x) = -\Big[\frac{1}{4}\delta(x - 0^+) + (4x^2 + \pi^2)^{-1}\Big].$$

This correction is in the following used to evaluate the correction to the average heat conductance of the SNS junction

$$\delta\kappa_{\mathrm{SNS}} = \int_0^\infty dx \kappa_{\mathrm{SNS}} \delta\rho(x). \tag{3.15}$$

Therefore the weak localization is defined as a negative correction to the average of heat conductance and it is of order $\mathcal{N}^0$ compared to the previously calculated $\langle\kappa_{\mathrm{SNS}}\rangle$, which is of order $\mathcal{N}$. The weak localization correction is hence expected to be of importance in particular in devices with a rather small amount of channels, such as in recently developed hybrid superconductor, semiconductor devices [49]. We show results for $\delta\kappa_{\mathrm{SNS}}$ in Fig. 3.6, which as expected have the order of magnitude of a single-channel heat conductance. Importantly, we see that the weak-localization correction re-establishes a dependence on the superconductors' phase

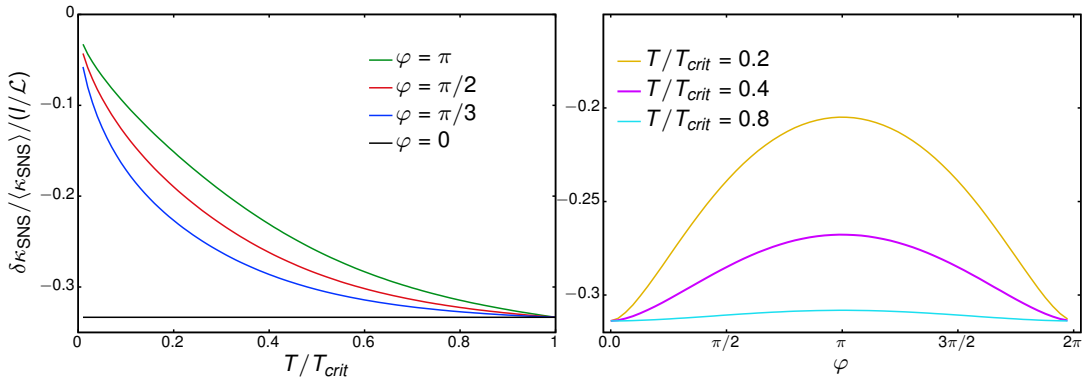

Figure 3.6: *Temperature- and phase-dependence of the weak localization correction* $\delta\langle\kappa_{SNS}\rangle$ *to the average heat conductance. (Left)* $\delta\kappa_{SNS}/\langle\kappa_{SNS}\rangle/(l/\mathcal{L})$ *as function of temperature* T/T_{crit} *at different phase differences* φ *and (Right) as function of the phase difference* φ *at different temperatures* T/T_{crit}*. The length scale is considered* $l/\mathcal{L} = 0.3$*.*

difference φ. This is intuitively clear since the weak localization itself arises from quantum-mechanical interference effects. The overall magnitude of $\delta\kappa_{\rm SNS}$ as a function of temperature depends on φ, as one can clearly see from panel (a) of Fig. 3.6. The phase dependence is most pronounced for smaller temperatures, $T/T_{\rm crit} \lesssim 0.5$. This correction is constant at zero phase when it is normalized to the average of conductance. This occurs because the zero phase transmission probability is equal to the transmission in normal metal which makes the ratio of the correction to the average to be temperature independent.

3.4 Universal conductance fluctuations

As we have seen so far in previous sections, transport properties such as charge and heat conductances are dependent to the transmission eigenvalues. In a normal metal this dependence is

$$G_{\rm N} = G_0 \sum_n D_n(\mu), \quad \kappa_{\rm N} = \kappa_0 \sum_n D_n(\mu), \tag{3.16}$$

where the quantum of charge and heat conductances are G_0 and κ_0. The transmission eigenvalues depend on energy. In the linear response regime, the applied voltage is much smaller than the typical energy scale of this dependence. Therefore D_n can be evaluated at the Fermi level. As we see in Eq. (3.16), in normal metals the transmission of transport channels contributes to the electrical conductance basically in the same way as to the thermal conductance; therefore thermal conductance fluctuations are expected to have similar properties. This is different in superconductors.

We want to address the variance of the heat conductance. Thanks to the eigenchannel decomposition of the full transmission matrix, leading to Eq. (3.4), the

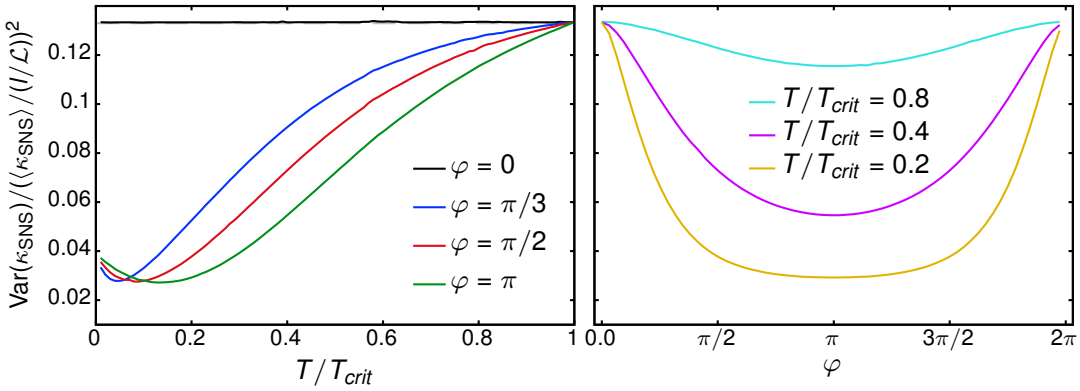

Figure 3.7: *Temperature- and phase-dependence of the heat conductance fluctuations* $Var[\kappa_{SNS}] / (\langle\kappa_{SNS}\rangle/(l/\mathcal{L}))^2$. *(Left)* $Var[\kappa_{SNS}] / (\langle\kappa_{SNS}\rangle/(l/\mathcal{L}))^2$ *as function of* T *for different* φ. *The black line at* $2/15$ *represents the normalconducting result, see Eq. (3.18a). (Right)* $Var[\kappa_{SNS}] / (\langle\kappa_{SNS}\rangle/(l/\mathcal{L}))^2$ *as function of* φ *for different* T*s.*

variance $\mathrm{Var}[\kappa_{\mathrm{SNS}}]$ can be directly computed as in Ref. [23, 48]

$$\mathrm{Var}\left[\kappa_{\mathrm{SNS}}\right] = \frac{1}{2\pi^2}\int_0^\infty dx \int_0^\infty dx' \left(\frac{d\kappa_{\mathrm{SNS}}(x)}{dx}\right) \times \left(\frac{d\kappa_{\mathrm{SNS}}(x')}{dx'}\right) \ln\left(\frac{1+\pi^2(x-x')^{-2}}{1+\pi^2(x+x')^{-2}}\right), \tag{3.17}$$

using the previously introduced parametrization of $D_n(x)$. Importantly, this term is of order $\mathcal{N}^0$. For the conductance $G/(e^2/h)$ of a normal-conducting junction in the diffusive limit, it takes the *universal* value $\mathrm{Var}\left[G/(e^2/h)\right] = 2/15$ for the type of system we are considering here. In particular, this means that the variance of the heat conductance of the *normal-conducting* junction $\kappa_{\mathrm{N}} = \kappa_0 \sum_{n=0}^{\mathcal{N}} D_n$, which, similarly to the conductance G, is simply linearly proportional to the average transmission, is given by

$$\mathrm{Var}\left[\frac{\kappa_{\mathrm{N}}}{\kappa_0}\right] = \frac{2}{15} \tag{3.18a}$$

$$\Rightarrow \mathrm{Var}\left[\kappa_{\mathrm{N}}\right] = \frac{2}{15}\left(\frac{\pi^2 k_{\mathrm{B}}^2}{3h}\right)^2 T^2. \tag{3.18b}$$

This quantity is hence universal up to a factor T^2, which is expected for the heat conductance (having a temperature dependent heat conductance quantum κ_0).

Also the fluctuations of the heat conductance of the SNS junction $\mathrm{Var}\left[\kappa_{\mathrm{SNS}}/\kappa_0\right]$ are of the order $\mathcal{N}^0$. However, in contrast to the straightforward result for the heat conductance fluctuations of the normal-junction, Eq. (3.18a), the phase difference across the SNS junctions induces a small, but nontrivial dependence of $\mathrm{Var}\left[\kappa_{\mathrm{SNS}}/\kappa_0\right]$ on phase and temperature.

4 Normal Metal as Heat Sink for Superconducting Devices

This chapter deals with the study of heat transport in normal-superconducting (NS, NIS or NNS) junctions. NS junctions are significant structures in the research of cooling. The energy gap in the superconducting electronic density of states, which is one of the defining properties of superconductors, can act as an energy filter for electrons. This property can be exploited in order to cool the superconducting lead in the junction via the normal conductor, acting as a heat sink, or vice versa.

In this chapter, we study heat transport in diffusive NS junctions. We use the same formalism as in Chapter 3 to construct the scattering matrix of a diffusive NS junction and to then calculate the heat conductance and its channel average using the Dorokhov formula. The results presented in this chapter constitute the starting point for further investigations of cooling in NS junctions.

4.1 Scattering Matrix of NS Junction

We first construct the scattering matrix of an NS junction. We employ the same trick as we used in Chapter 3 for an SNS junction, formally dividing the junction into NN and an NS subjunctions. We assume a disordered region in the normal conducting junction as shown in Fig. (4.1) and write the scattering matrix of the whole NS junction in terms of the normal scattering matrix of this region.

We first write down the scattering matrix of the NS and NN junction separately, and next, combine them to have the scattering matrix of the whole junction. The reflection and transmission coefficients in the NS interface are calculated by wave function matching in Appendix B. Here are the results of these coefficients

$$r_{eh} = \frac{u_0 v_0}{\gamma}, \tag{4.1a}$$

$$r_{ee} = -\frac{(u_0^2 - v_0^2)(Z^2 + iZ)}{\gamma}, \tag{4.1b}$$

$$t_{eh} = \frac{iv_0 Z}{\gamma}, \tag{4.1c}$$

$$t_{ee} = \frac{u_0}{\gamma}(1 - iZ), \tag{4.1d}$$

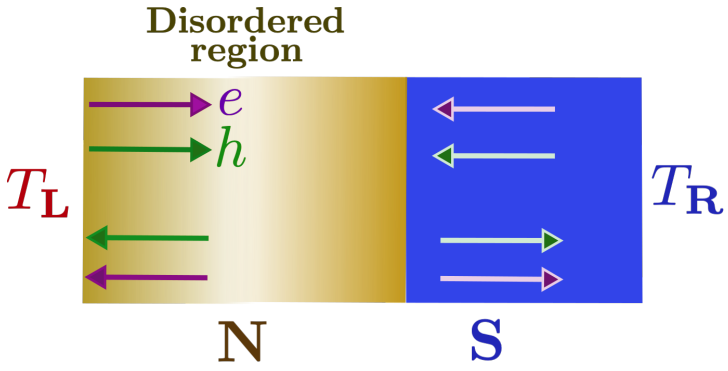

Figure 4.1: *Normal-metal-superconducting (NS) junction containing a disordered normal region. Scattering states in both normal and superconducting leads are indicated schematically.*

where $Z = mH/\hbar^2 k_F$ corresponds to an effective barrier at the interface of a normal metal and a superconductor, H stands for the potential of this barrier and $\gamma = u_0^2 + (u_0^2 - v_0^2)Z^2$ [50].

In Eqs. (4.1), r_{eh} corresponds to the Andreev reflection, r_{ee} to ordinary reflection, t_{ee} to transmission without branch crossing and t_{eh} to transmission with crossing between electron and hole branches. Due to the conservation of probability, the sum of related probabilities to all of these coefficients is one. In the absence of a barrier [that is, when $H = 0$], one gets $Z = 0$ and consequently $r_{ee} = t_{eh} = 0$. In this case there are two regimes, the first one for $E < \Delta$ (i.e., for energies below the superconductor gap) where $t_{ee} = 0$, and the only possible scattering is Andreev reflection with the probability of $A = r_{eh}^* r_{eh} = 1$. The second case is for energies above the gap, $E > \Delta$, in which there is both Andreev reflection and transmission without branch crossing in the absence of a barrier. Using Eqs. (4.1) for energies above the superconductor gap in the absence of a barrier, the scattering matrix of the NS interface can be written as follows:

$$
\begin{aligned}
S_{\mathrm{NS}} &= \frac{1}{u}\begin{bmatrix} 0 & \sqrt{\xi/E}e^{i\varphi/2} & ve^{i\varphi} & 0 \\ \sqrt{\xi/E}e^{-i\varphi/2} & 0 & 0 & -v \\ ve^{-i\varphi} & 0 & 0 & \sqrt{\xi/E}e^{-i\varphi/2} \\ 0 & -v & \sqrt{\xi/E}e^{i\varphi/2} & 0 \end{bmatrix} \\
&= \begin{bmatrix} 0 & \cos\alpha e^{i\varphi/2} & \sin\alpha e^{i\varphi} & 0 \\ \cos\alpha e^{-i\varphi/2} & 0 & 0 & -\sin\alpha \\ \sin\alpha e^{-i\varphi} & 0 & 0 & \cos\alpha e^{-i\varphi/2} \\ 0 & -\sin\alpha & \cos\alpha e^{i\varphi/2} & 0 \end{bmatrix},
\end{aligned}
\tag{4.2}
$$

where we have introduced the angle α defined as $\sin\alpha = v/u$. The scattering matrix satisfies the time-reversal and particle-hole symmetry [37]. Since in an NS junction there is only one superconductor, there is no phase difference between

different superconductors, and φ can be set to zero which does not make any difference in calculating transmission probabilities.

The scattering matrix of the normal region, as we saw in previous chapters, can be written in terms of the transmission probabilities of the disordered normal region. The structure of this normal scattering matrix is

$$S_{\mathrm{N}} = \begin{bmatrix} s_0(\varepsilon) & 0 \\ 0 & s_0(-\varepsilon)^\dagger \end{bmatrix}. \tag{4.3}$$

Using the polar decomposition [23], the matrix $s_0(\varepsilon)$ is written as

$$s_0 = \begin{bmatrix} U_1 & \mathbf{0} \\ \mathbf{0} & U_2 \end{bmatrix} \begin{bmatrix} \sqrt{1-\mathbf{D}} & \sqrt{\mathbf{D}} \\ \sqrt{\mathbf{D}} & -\sqrt{1-\mathbf{D}} \end{bmatrix} \begin{bmatrix} V_1 & \mathbf{0} \\ \mathbf{0} & V_2 \end{bmatrix}, \tag{4.4}$$

where $\mathbf{D}$ is a diagonal matrix of normal transmissions D_n and U_1, U_2, V_1, V_2 are four $N \times N$ unitary matrices.

4.1.1 Transmission Probabilities

Combining the scattering matrix of the NS interface with the normal scattering matrix we obtain the transmission probabilities of the whole NS junction illustrated in Fig. (4.1). The transmission probability of an electronic state is the sum $\mathcal{D}^e = \mathcal{D}_n^{ee} + \mathcal{D}_n^{eh}$.

$$\mathcal{D}_n^{ee} = \frac{D_n \cos^2\alpha}{(1-(1-D_n)\sin^2\alpha)^2} \tag{4.5a}$$

$$\mathcal{D}_n^{eh} = \frac{\sin^2\alpha\, \cos^2\alpha\, D_n(1-D_n)}{(1-(1-D_n)\sin^2\alpha)^2}, \tag{4.5b}$$

where

$$\cos^2\alpha = \frac{2\xi}{E+\xi} \quad \text{and} \quad \sin^2\alpha = \frac{\Delta^2}{(E+\xi)^2}. \tag{4.6}$$

Here, $\mathcal{D}_n^e$ and $\mathcal{D}_n^h$, which are equivalently obtained from $\mathcal{D}_n^{hh} + \mathcal{D}_n^{he}$, denote transmission probabilities for electrons and holes, and as a consequence of the particle and hole symmetry they fulfill $\mathcal{D}_n^e = \mathcal{D}_n^h$. The transmission probabilities depend on the superconductor's gap.

4.2 Heat Current and Heat Conductance

As discussed in Chapter 3, the heat current in the superconducting lead has two parts for electrons and holes

$$J(T) = \frac{1}{h}\sum_{n=0}^{\mathcal{N}} \int_0^\infty dE\, E\, \Big[\mathcal{D}_n^e(E) + \mathcal{D}_n^h(E)\Big]\Big[f_{\mathrm{L}}(E) - f_{\mathrm{R}}(E)\Big]. \tag{4.7}$$

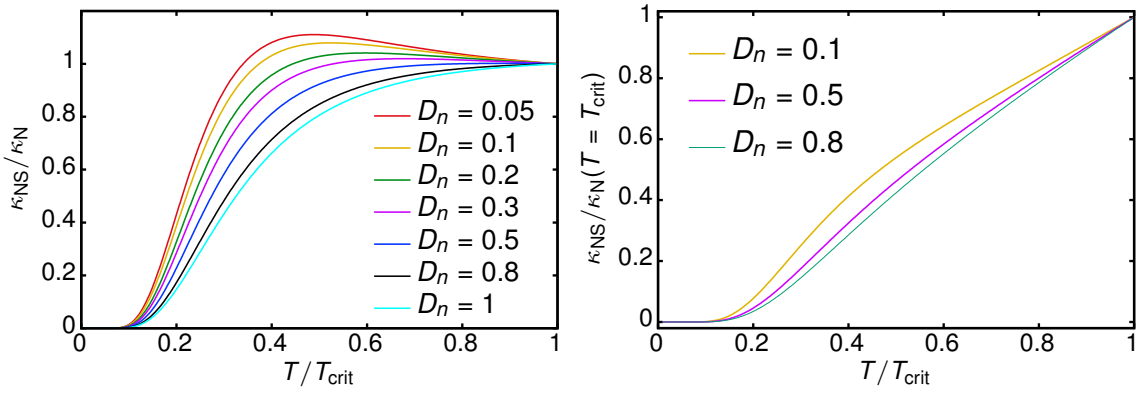

Figure 4.2: *Temperature dependence of single channel heat conductance of an NS junction at different transmissions of the disordered normal region. At $T = T_{crit}$ the heat conductance becomes equal to the normal heat conductance. In the left panel the normal heat conductance, κ_N, with respect to which κ_{NS} is normalized, is temperature dependent and in the right panel the conductance is normalized to the normal heat conductance at T_{crit}.*

The heat current depends also on the difference between Fermi functions of the left and right leads of the NNS junction. In the linear response regime, when the temperature difference between the left and right leads is small, we obtain heat conductance from heat current. By employing

$$f_{\rm L}(E) - f_{\rm R}(E) \approx \frac{E}{4\cosh^2(E/2K_BT)k_BT^2}\delta T, \tag{4.8}$$

together with Eq. (4.5), and considering linear response regime $J(T) = \kappa_{\rm NS}(T)\delta T$, we obtain the heat conductance of an NS junction

$$\kappa_{\rm NS}(T) = \frac{1}{2hk_BT^2}\sum_{n=0}^{\mathcal{N}}\int_0^\infty dE\,\frac{E^2}{\cosh^2(E/k_BT)} \times \frac{\cos^2\alpha D_n(1+\sin^2\alpha(1-D_n))}{(1-(1-D_n)\sin^2\alpha)^2}. \tag{4.9}$$

? The temperature dependent heat conductance of NNS junction is shown in Fig. (4.2) for a single channel at different normal transmissions. The single cha?nnel conductance compared to the normal conductance have similar behavior in NS and SNS junctions by having a larger value for conductances at some temperatures below $T_{\rm crit}$. The single channel conductance which is normalized to the conductance at $T_{\rm crit}$ shows the same behavior to the results of a previous experiment [51]. The average NS heat conductance is shown in Fig. (4.3). The averaging is calculated using the same formalism as that introduced in Chapter 3 for averaging the SNS conductance. The SNS results are highly φ dependent. It seems that $\Delta_{\rm L} \neq \Delta_{\rm R}$ can lead to $\kappa_{\rm NS/SNS} > \kappa_{\rm N}$ even at $\varphi = 0$. The behavior of

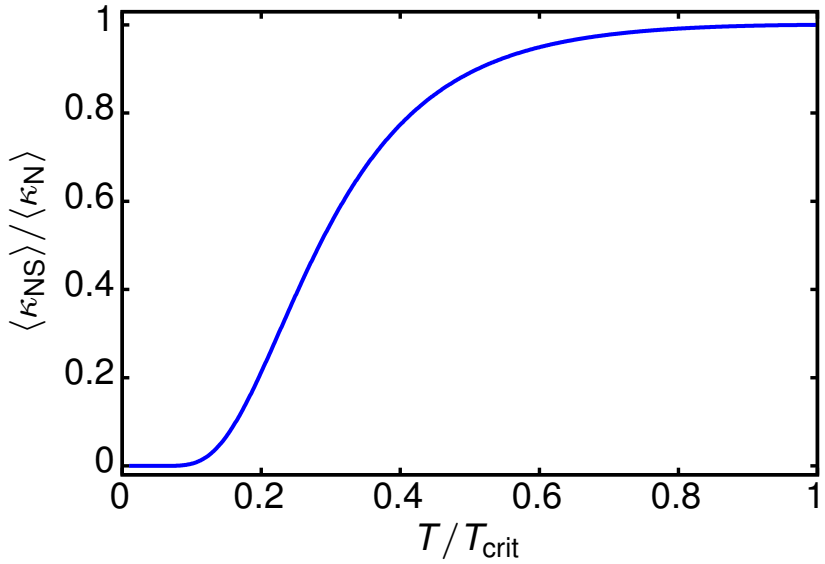

Figure 4.3: *Temperature dependent of the average heat conductance of NS junction normalized to the average of normal heat conductance.*

$\langle \kappa_{\mathrm{NS}} \rangle$ is what we expect. For the SNS case, $\langle \kappa_{\mathrm{SNS}} \rangle$ depended only on $\Delta_{\max}$ and not on φ. Therefore this should be the same for NS.

4.3 Phonon Heat Transport

One of the questions that becomes important when thinking of applications is the contribution of phonons comparing to quasiparticles in the heat conductance of superconducting junctions. In general, it is not straightforward to separate the lattice and quasiparticle components of heat conductance in superconductors. This is due to the influence of quasiparticles on the lattice contribution of heat conductance through electron-phonon coupling. There have been observed various results in different experiments for the comparison of quasiparticle and phonon heat conductances. One of the experiments on measuring the thermal conductance of a superconductor has been performed in a temperature range where lattice conduction dominates [52]. This kind of measurements are still limited due to the scattering of phonons by electrons. It has been shown in another experiment that a finite electron-phonon coupling would lead to an increase in lattice conductance below the critical temperature T_{crit} of superconductor [53]. Therefore it seems to be an important question to what extent the phonon contribution to heat conductance is noticeable and how electron-phonon coupling affects the contribution of both lattice and quasiparticles to heat conductance.

5 Summary

In this thesis we discuss heat transport in superconducting hybrid structures. In order to investigate the influence of superconductivity on heat transport in temperature-biased systems, we study two types of structures, containing superconducting elements as well as normal conductors. The first structure is a Josephson junction containing a normal disordered scattering region between two superconductors. In addition to the temperature bias, there is also a crucially important phase difference between the superconducting condensates of the two contacts and the two superconductors of the SNS junction can have different gaps. In the second structure, an SN junction, one of the superconducting contacts is replaced by a normal conductor.

We analyze the behavior of thermal properties such as the linear-response heat conductance and in particular the influence, which the junction properties have on the heat transport. The disordered region of the junction, which we consider here, is characterized by a large number $\mathcal{N}$ of transport channels with randomly distributed transmission probabilities. As a consequence, we consider the channel-averaged heat conductance, which turns out to be independent of the superconducting phases and only governed by temperature compared to the largest of the superconducting gaps in the structure. In addition, we calculate the weak localization correction of the heat conductance. Finally, we address the heat conductance fluctuations. We find these heat conductance fluctuations to have a similarly universal behavior as the well known charge conductance fluctuations. However, we can also identify an up-to-date unknown, non-trivial dependence on the superconducting phase in SNS junctions. In order to analyze the heat transport in these junctions, we use a Landauer-Büttiker scattering theory for quasiparticle excitations in the superconductor together with previously obtained distribution functions for disordered junctions from random-matrix theory.

After a general overview in Chapter 1, we introduce the scattering formalism for heat transport in Chapter 2, both for fully normal-conducting systems, as well as for hybrid superconducting systems, described by Bogoliubov-de Gennes equations. In order to calculate the heat current or the heat conductance, the full scattering matrix of the structure of interest is required.

In Chapter 3 and in the Appendices, we show a detailed derivation of the scattering matrix of an SNS junction. This is done by combining the scattering matrices of SN junctions—obtained from wave-function matching using Bogoliubov-de Gennes equations—with the scattering matrix of the disordered normal region.

We write the scattering matrix S_{N} of the normal-conducting disordered region in terms of the transmission eigenvalues (D_n) using a polar decomposition. As a result, we obatin the scattering matrix of the whole SNS junction in terms of these transmission eigenvalues of S_{N}. This approach is beneficial, since we can directly employ the statistical distribution of the transmission eigenvalues of the normal region to get a channel-average of the heat conductance of the full SNS structure. The obtained scattering matrix of the SNS junction is valid for arbitrary junction transmission D_n, as well as for superconductors with different gaps and phases. It can therefore serve as the starting point for the analysis of both types of structures, SNS and SN, which we are interested in in this thesis.

In the second part of Chapter 3, we then use the obtained matrix to calculate the heat current and the heat conductance in the linear response regime for the SNS junction. Importantly, the heat conductance is phase-dependent, as it has recently experimentally been observed in Josephson heat interferometers [9]. In order to investigate the effect of the disordered region on the heat conductance, we use the so-called Dorokhov distribution, which proposes a bimodal density distribution for the transmission eigenvalues D_n. Using this distribution we calculate the averaged heat conductance in the SNS junction and find that, surprisingly, the disorder averaging fully suppresses the phase dependence of the heat conductance. Considering the length of the disordered junction in the SNS structure to be much smaller than the localization length of electrons, that is the number of channels multiplied by the electron mean free path ($\mathcal{N}l$), we expect weak localization to occur in the normal junction. Calculating this $\mathcal{N}$-independent weak localization correction to the average heat conductance, we notice that a dependence on the superconducting phase-difference is restored.

Finally, we address the variance of the statistics of the heat conductance. These heat conductance fluctuations can be studied employing the same formalism, which we used for averaging and weak localization, the DMPK formalism. The heat conductance fluctuations —being a quantum effect— are again phase-dependent in an SNS junction, in contrast to the average heat conductance. Interestingly, we furthermore find that the heat conductance fluctuations are similarly universal as the famous universal conductance fluctuations of charge currents. These fluctuations are independent of the junction length and of order unity, when compared to the (heat) conductance average.

In the end in Chapter 4 we describe the heat current and conductance in an NS junction with the same formalism of the previous chapters. This analysis is mostly motivated by the interest in NS junctions for cooling applications. Also here we find that the statistics of the transmission eigenvalues of the disordered region lead to sensitive differences in the heat conductance with respect to results obtained for single-channel junctions.

Outlook

In this thesis, we set up a scattering matrix formalism for the heat conductance of hybrid superconducting devices. With this formalism at hand, we are now able to consider further, experimentally relevant hybrid structures, where (1) a complex junction design can be taken into account (2) multi-terminal structures can be considered and (3) higher-order correlation functions can straightforwardly be addressed.

It is of particular interest to compare the magnitude of the heat current noise [54] (the second-order correlation function between heat currents) to the variance of the heat current statistics due to the distribution of transmission probabilities in a disordered region. The calculation of the heat current noise using the scattering matrix approach is a currently ongoing project.

Finally, we have briefly addressed the question of phononic heat transport in Chapter 4. Phononic heat transport is largely suppressed in low-temperature experiments. However, in particular in applications of NS junction in cooling, this contribution is expected to be of relevance. Also here, we are interested in comparing the order of magnitude of effects calculated in this thesis to effects of phonon scatterings and electron-phonon interactions in heat transport in NS junctions.

Appendices

Appendix A

Heat current operator in superconductors

Heat current is defined as the difference of energy currents of particles with respect to the energy current at the Fermi level

$$J = I^E - \mu I^P. \tag{A.1}$$

Therefore in order to calculate the heat current we need the energy current. We start with the density of energy flow for which we write the corresponding continuity equation so that the following conservation law holds

$$\frac{\partial \rho^E}{\partial t} + \vec{\nabla} \dot{j}^E = \rho_S^E. \tag{A.2}$$

Here, j^E is the energy current density and ρ^E is the energy density. The current is injected into the system by a source and ρ_S^E is the energy density of the source. The expectation value of the energy of a particle described by the Hamiltonian $H = -\hbar^2\vec{\nabla}^2/(2m)$ is given by

$$\langle E \rangle = -\frac{\hbar^2}{2m} \sum_i \int_v dv\, \psi_\alpha^\dagger(\vec{r},t)\vec{\nabla}^2\psi_\alpha(\vec{r},t), \tag{A.3}$$

where the sum is over all leads i and the integration is over the entire volume of the system. The time derivative of this average is

$$\frac{\partial}{\partial t}\langle E \rangle = -\frac{\hbar^2}{2m} \sum_i \int_v dv \left\{ \vec{\nabla} \cdot \left[\frac{\partial}{\partial t}\left(\psi_i^\dagger \vec{\nabla}\psi_i\right)\right] - \frac{\partial}{\partial t}\left(\vec{\nabla}\psi_\alpha^\dagger \vec{\nabla}\psi_\alpha\right)\right\}. \tag{A.4}$$

Using that

$$\vec{\nabla} \cdot \left[\frac{\partial \psi_\alpha^\dagger}{\partial t}\vec{\nabla}\psi_\alpha + \vec{\nabla}\psi_\alpha^\dagger \frac{\partial \psi_\alpha}{\partial t}\right] = \frac{\partial}{\partial t}\left(\vec{\nabla}\psi_\alpha^\dagger \vec{\nabla}\psi_\alpha\right), \tag{A.5}$$

one can reformulate Eq. (A.4) as follows:

$$\frac{\partial}{\partial t}\langle E \rangle = -\frac{\hbar^2}{2m} \sum_\alpha \int_v dv\, \vec{\nabla} \cdot \left[\psi_\alpha^\dagger \frac{\partial \psi_\alpha}{\partial t} - \vec{\nabla}\psi_\alpha^\dagger \frac{\partial \psi_\alpha}{\partial t}\right]. \tag{A.6}$$

Thereby the energy current density can be written as

$$j_\alpha^E(\vec{r},t) = \frac{\hbar^2}{2m}\Big[\psi_\alpha^\dagger(\vec{r},t)\frac{\partial\vec{\nabla}\psi_\alpha(\vec{r},t)}{\partial t} - \vec{\nabla}\psi_\alpha^\dagger(\vec{r},t)\frac{\partial\psi_\alpha(\vec{r},t)}{\partial t}\Big]. \tag{A.7}$$

The total energy current along the chosen axis (here x_α) is found then by integrating out Eq. (A.7) with respect to the transverse cross-section through which the current flows,

$$I_\alpha^E(x_\alpha,t) = \int dy_\alpha\, dz_\alpha\, j_\alpha^E(\vec{r}_\alpha,t). \tag{A.8}$$

Replacing the wave functions with the field operators in the above formula gives the energy current operator.

The wave functions in a superconductor are a combination of electron-like and hole-like quasipartricles:

$$\psi_e(x) = \begin{bmatrix} ue^{-i\varphi/2} \\ ve^{i\varphi/2} \end{bmatrix} e^{\pm ik^+x} \tag{A.9a}$$

$$\psi_h(x) = \begin{bmatrix} ve^{-i\varphi/2} \\ ue^{i\varphi/2} \end{bmatrix} e^{\mp ik^-x}. \tag{A.9b}$$

The wave vectors k^+ and k^- represent the wave vectors of electron- and hole-like quasiparticles in a superconductor which are calculated using Bogoliubov-De Gennes equation in Chap. 2. The total wave function written in terms of electron- and hole-like wave functions and with the amplitudes replaced by field operators takes the form

$$\psi_\alpha(\vec{r},t) = \hat{a}_e \begin{bmatrix} ue^{-i\varphi/2} \\ ve^{i\varphi/2} \end{bmatrix} e^{-ik^+x} + \hat{b}_e \begin{bmatrix} ue^{-i\varphi/2} \\ ve^{i\varphi/2} \end{bmatrix} e^{ik^+x} + \hat{a}_h \begin{bmatrix} ve^{-i\varphi/2} \\ ue^{i\varphi/2} \end{bmatrix} e^{ik^-x} + \hat{b}_h \begin{bmatrix} ve^{-i\varphi/2} \\ ue^{i\varphi/2} \end{bmatrix} e^{-ik^-x}. \tag{A.10}$$

Inserting this wave function into Eq. (A.7) We obtain the total energy current operator

$$\hat{I}^E(t,T)_{\alpha,\mathrm{S}} = \frac{1}{h}\sum_n^{\mathcal{N}}\sum_{i=e,h}\int_\Delta^\infty dE\, dE'\, e^{i(E-E')t/\hbar} \times \frac{E+E'}{2}\Big[\hat{\mathrm{b}}_{i,n}^\dagger(E)\hat{\mathrm{b}}_{i,n}(E') - \hat{\mathrm{a}}_{i,n}^\dagger(E)\hat{\mathrm{a}}_{i,n}(E')\Big]. \tag{A.11}$$

Here, $\hat{a}_{i,n}^\dagger$ ($\hat{a}_{i,n}$) and $\hat{b}_{i,n}^\dagger$ ($\hat{b}_{i,n}$) are creation (annihilation) operators for electron-like and hole-like quasiparticles which are called Boholiubov operators. This energy-current operator consists of two parts for electron- and hole-like quasiparticles. If we assume the Fermi level to be set at zero $\mu = 0$, the formula for the heat current (2.19) is identical to that for the energy current (A.11).

Appendix B

Transmission and reflection coefficients in NS junction

In this appendix we derive transmission and reflection coefficients in an NS junction. Assuming that particles travel from N to S, appropriate boundary conditions for these particles can be formulated as follows:
(i) Continuity of wave function ψ at $x = 0$, so that

$$\psi_N(0) = \psi_S(0) \equiv \psi(0). \tag{B.1}$$

(ii) The derivative boundary condition appropriate for the Dirac-δ potential

$$\frac{\hbar^2}{2m}\left[\frac{\partial\psi_S(x)}{\partial x} - \frac{\partial\psi'_N(x)}{\partial x}\right] = H\psi(0). \tag{B.2}$$

Next, using the incident (ψ_{inc}), reflected (ψ_{ref}) and transmitted (ψ_{trans}) components of a wave function,

$$\psi_{inc} = \begin{bmatrix} 1 \\ 0 \end{bmatrix} e^{iq^+x}, \quad \text{with } \hbar q^{\pm} = \sqrt{2m(\mu \pm E)}, \tag{B.3a}$$

$$\psi_{ref} = a\begin{bmatrix} 0 \\ 1 \end{bmatrix} e^{iq^-x} + b\begin{bmatrix} 1 \\ 0 \end{bmatrix} e^{-iq^+x}, \tag{B.3b}$$

$$\psi_{trans} = c\begin{bmatrix} u_0 \\ v_0 \end{bmatrix} e^{ik^+x} + d\begin{bmatrix} v_0 \\ u_0 \end{bmatrix} e^{-ik^-x}, \tag{B.3c}$$

the wave functions in the normal (ψ_N) and superconducting (ψ_S) part of the junction can be written as:

$$\psi_N = \psi_{inc} + \psi_{refl} = \begin{bmatrix} 1 \\ 0 \end{bmatrix} e^{iq^+x} + a\begin{bmatrix} 0 \\ 1 \end{bmatrix} e^{iq^-x} + b\begin{bmatrix} 1 \\ 0 \end{bmatrix} e^{-iq^+x}, \tag{B.4a}$$

$$\psi_S = \psi_{trans} = c\begin{bmatrix} u_0 \\ v_0 \end{bmatrix} e^{ik^+x} + d\begin{bmatrix} v_0 \\ u_0 \end{bmatrix} e^{-ik^-x}. \tag{B.4b}$$

Furthermore, the relevant derivatives of such wave functions are:

$$\psi'_N = \frac{\partial \psi_N}{\partial x} = iq^+ \begin{bmatrix} 1 \\ 0 \end{bmatrix} e^{iq^+ x} + iq^- a \begin{bmatrix} 0 \\ 1 \end{bmatrix} e^{iq^- x} - iq^+ b \begin{bmatrix} 1 \\ 0 \end{bmatrix} e^{-iq^+ x}, \tag{B.5a}$$

$$\psi'_S = \frac{\partial \psi_S}{\partial x} = ik^+ c \begin{bmatrix} u_0 \\ v_0 \end{bmatrix} e^{ik^+ x} - ik^- d \begin{bmatrix} v_0 \\ u_0 \end{bmatrix} e^{-ik^- x}, \tag{B.5b}$$

where $k^+ = k^- = q^+ = q^- = k_F$. From the first boundary condition (B.1) we then obtain:

$$\begin{bmatrix} 1 \\ 0 \end{bmatrix} + a \begin{bmatrix} 0 \\ 1 \end{bmatrix} + b \begin{bmatrix} 1 \\ 0 \end{bmatrix} = c \begin{bmatrix} u_0 \\ v_0 \end{bmatrix} + d \begin{bmatrix} v_0 \\ u_0 \end{bmatrix} \tag{B.6}$$

together with

$$1 + b = cu_0 + dv_0 \quad \text{and} \quad a = cv_0 + du_0. \tag{B.7}$$

Analogously, we apply the second boundary condition (B.2):

$$\frac{\hbar^2}{2m} ik_F \left(c \begin{bmatrix} u_0 \\ v_0 \end{bmatrix} - d \begin{bmatrix} v_0 \\ u_0 \end{bmatrix} - \begin{bmatrix} 1 \\ 0 \end{bmatrix} - a \begin{bmatrix} 0 \\ 1 \end{bmatrix} + b \begin{bmatrix} 1 \\ 0 \end{bmatrix} \right) = H \left(\begin{bmatrix} 1 \\ 0 \end{bmatrix} + a \begin{bmatrix} 0 \\ 1 \end{bmatrix} + b \begin{bmatrix} 1 \\ 0 \end{bmatrix} \right) \tag{B.8}$$

so that

$$\frac{i\hbar^2 k_F}{2m}(cu_0 - dv_0 - 1 + b) = H(1 + b) = H(cu_0 + dv_0), \tag{B.9a}$$

$$\frac{i\hbar^2 k_F}{2m}(cv_0 - du_0 - a) = Ha = H(cv_0 + du_0). \tag{B.9b}$$

From Eqs. (B.9) one can find:

$$c = \frac{-u_0}{Hv_0} \left(H + \frac{i\hbar^2 k_F}{m} \right) d, \tag{B.10a}$$

$$d = iv_0 \frac{mH/\hbar^2 k_F}{u_0^2 + (u_0^2 - v_0^2)(mH/\hbar^2 k_F)^2}. \tag{B.10b}$$

We note that by introducing the auxiliary notation

$$Z = \frac{mH}{\hbar^2 k_F} \quad \text{and} \quad \gamma = u_0^2 + (u_0^2 - v_0^2) Z^2, \tag{B.11}$$

Eqs. (B.10) can be further simplified:

$$d = \frac{iv_0 Z}{\gamma} \quad \text{and} \quad c = \frac{u_0}{\gamma}(1 - iZ). \tag{B.12}$$

It is not clear where the following equations come from. From Eqs. (??) one also finds:

$$a = cv_0 + du_0 = \frac{u_0 v_0}{\gamma}, \tag{B.13a}$$

$$b = cu_0 + dv_0 - 1 = -\frac{(u_0^2 - v_0^2)(Z^2 + iZ)}{\gamma}. \tag{B.13b}$$

In fact, the coefficients above represent transmission and reflection amplitudes, that is, a describes the Andreev reflection (i.e., reflection with branch crossing), b is associated with the ordinary reflection, c corresponds to transmission without branch crossing, while d to transmission with branch crossing. The related probabilities are A, B, C, and D, and there is conservation of probability as $A(E) + B(E) + C(E) + D(E) = 1$. These probabilities are actually the probability currents for the particle.

In the absence of a barrier [namely, for $H = 0$] one finds $Z = 0$, and thus, $b = d = 0$. In such a case, we can distinguish two situations: the first one for $E < \Delta$ (i.e., for energies below the gap of superconductor) when $c = 0$ and there is just Andreev reflection with the probability of $A = |a|^2 = 1$. On the other hand, the second situation corresponds to $E > \Delta$ (i.e., there is effectively no barrier), so that all reflections are Andreev reflections and all transmissions occur without branch crossing.

Appendix C

Scattering matrix of SNS junction

We shall prove the derivation of scattering matrix of an SNS junction. The model we consider is shown schematically in Fig. 3.1. We start from the scattering matrix of SN junction. As it is shown in Appendix (B) by performing the wave function matching of normal and superconducting region, one can obtain the scattering matrix of SN junction. In our model there are three sub junctions: $S_L N_L$, $N_L N_R$ and $N_R S_R$. The incoming and outgoing states associated with these three junctions are related by scattering matrices as follows:

$$\begin{bmatrix} \hat{b}_e(S_L) \\ \hat{b}_e(N_L) \\ \hat{b}_h(S_L) \\ \hat{b}_h(N_L) \end{bmatrix} = \begin{bmatrix} 0 & \cos\alpha e^{-i\varphi_L/2} & -\sin\alpha & 0 \\ \cos\alpha e^{i\varphi_L/2} & 0 & 0 & \sin\alpha e^{i\varphi_L} \\ -\sin\alpha & 0 & 0 & \cos\alpha e^{i\varphi_L/2} \\ 0 & \sin\alpha e^{-i\varphi_L} & \cos\alpha e^{-i\varphi_L/2} & 0 \end{bmatrix} \begin{bmatrix} \hat{a}_e(S_L) \\ \hat{a}_e(N_L) \\ \hat{a}_h(S_L) \\ \hat{a}_h(N_L) \end{bmatrix}, \tag{C.1}$$

$$\begin{bmatrix} \hat{a}_e(N_L) \\ \hat{a}_e(N_R) \\ \hat{a}_h(N_L) \\ \hat{a}_h(N_R) \end{bmatrix} = S_N \begin{bmatrix} \hat{b}_e(N_L) \\ \hat{b}_e(N_R) \\ \hat{b}_h(N_L) \\ \hat{b}_h(N_R) \end{bmatrix}, \tag{C.2}$$

$$\begin{bmatrix} \hat{b}_e(N_R) \\ \hat{b}_e(S_R) \\ \hat{b}_h(N_R) \\ \hat{b}_h(S_R) \end{bmatrix} = \begin{bmatrix} 0 & \cos\alpha e^{i\varphi_R/2} & \sin\alpha e^{i\varphi_R} & 0 \\ \cos\alpha e^{-i\varphi_R/2} & 0 & 0 & -\sin\alpha \\ \sin\alpha e^{-i\varphi_R} & 0 & 0 & \cos\alpha e^{-i\varphi_R/2} \\ 0 & -\sin\alpha & \cos\alpha e^{i\varphi_R/2} & 0 \end{bmatrix} \begin{bmatrix} \hat{a}_e(N_R) \\ \hat{a}_e(S_R) \\ \hat{a}_h(N_R) \\ \hat{a}_h(S_R) \end{bmatrix}, \tag{C.3}$$

Where $\sin\alpha = v/u$, $u = \sqrt{\Delta/2E}\, e^{\mathrm{arcosh}(E/\Delta)/2}$ and $v = \sqrt{\Delta/2E}\, e^{-\mathrm{arcosh}(E/\Delta)/2}$. Δ is the temperature dependent superconductor gap and we are interested in working at energies above the gap. φ is the phase difference between left and right superconductors. The aim is to express the SNS scattering matrix (S_{SNS}) in terms of the scattering matrix of the normal region (S_N). S_{SNS} relates the states

in S regions, so we should write all the states of N region in terms of S region's states. From eq. (C.1) we have:

$$\begin{aligned}
\hat{\mathrm{a}}_e(\mathrm{N_L}) &= \sec\alpha e^{i\varphi_\mathrm{L}/2}[\hat{\mathrm{b}}_e(\mathrm{S_L}) + \sin\alpha\hat{\mathrm{a}}_h(\mathrm{S_L})], \\
\hat{\mathrm{b}}_e(\mathrm{N_L}) &= \sec\alpha e^{i\varphi_\mathrm{L}/2}[\hat{\mathrm{a}}_e(\mathrm{S_L}) + \sin\alpha\hat{\mathrm{b}}_h(\mathrm{S_L})], \\
\hat{\mathrm{a}}_h(\mathrm{N_L}) &= \sec\alpha e^{i\varphi/2}[\hat{\mathrm{b}}_h(\mathrm{S_L}) + \sin\alpha\hat{\mathrm{a}}_e(\mathrm{S_L})], \\
\hat{\mathrm{b}}_h(\mathrm{N_L}) &= \sec\alpha e^{i\varphi/2}[\hat{\mathrm{a}}_h(\mathrm{S_L}) + \sin\alpha\hat{\mathrm{b}}_e(\mathrm{S_L})].
\end{aligned} \tag{C.4}$$

Similarly for $\mathrm{N_R S_R}$ junction by using Eq. (C.9) we have:

$$\begin{aligned}
\hat{\mathrm{a}}_e(\mathrm{N_R}) &= \sec\alpha e^{-i\varphi/2}[\hat{\mathrm{b}}_e(\mathrm{S_R}) + \sin\alpha\hat{\mathrm{a}}_h(\mathrm{S_R})], \\
\hat{\mathrm{b}}_e(\mathrm{N_R}) &= \sec\alpha e^{-i\varphi/2}[\hat{\mathrm{a}}_e(\mathrm{S_R}) + \sin\alpha\hat{\mathrm{b}}_h(\mathrm{S_R})], \\
\hat{\mathrm{a}}_h(\mathrm{N_R}) &= \sec\alpha e^{i\varphi/2}[\hat{\mathrm{b}}_h(\mathrm{S_R}) + \sin\alpha\hat{\mathrm{a}}_e(\mathrm{S_R})], \\
\hat{\mathrm{b}}_h(\mathrm{N_R}) &= \sec\alpha e^{i\varphi/2}[\hat{\mathrm{a}}_h(\mathrm{S_R}) + \sin\alpha\hat{\mathrm{b}}_e(\mathrm{S_R})].
\end{aligned} \tag{C.5}$$

Substituting Eqs. (C.4 and C.5) into Eq. (C.2) gives

$$\begin{aligned}
&\begin{bmatrix} e^{-i\varphi/2}\hat{\mathrm{b}}_e(\mathrm{S_L}) \\ e^{-i\varphi/2}\hat{\mathrm{b}}_e(\mathrm{S_R}) \\ e^{i\varphi/2}\hat{\mathrm{b}}_h(\mathrm{S_L}) \\ e^{i\varphi/2}\hat{\mathrm{b}}_h(\mathrm{S_R}) \end{bmatrix} + \sin\alpha \begin{bmatrix} e^{-i\varphi/2}\hat{\mathrm{a}}_h(\mathrm{S_L}) \\ e^{-i\varphi/2}\hat{\mathrm{a}}_h(\mathrm{S_R}) \\ e^{i\varphi/2}\hat{\mathrm{a}}_e(\mathrm{S_L}) \\ e^{i\varphi/2}\hat{\mathrm{a}}_e(\mathrm{S_R}) \end{bmatrix} = \\
&S_\mathrm{N}\left(\begin{bmatrix} e^{-i\varphi/2}\hat{\mathrm{a}}_e(\mathrm{S_L}) \\ e^{-i\varphi/2}\hat{\mathrm{a}}_e(\mathrm{S_R}) \\ e^{i\varphi/2}\hat{\mathrm{a}}_h(\mathrm{S_L}) \\ e^{i\varphi/2}\hat{\mathrm{a}}_h(\mathrm{S_R}) \end{bmatrix} + \sin\alpha \begin{bmatrix} e^{-i\varphi/2}\hat{\mathrm{b}}_h(\mathrm{S_L}) \\ e^{-i\varphi/2}\hat{\mathrm{b}}_h(\mathrm{S_R}) \\ e^{i\varphi/2}\hat{\mathrm{b}}_e(\mathrm{S_L}) \\ e^{i\varphi/2}\hat{\mathrm{b}}_e(\mathrm{S_R}) \end{bmatrix} \right)
\end{aligned} \tag{C.6}$$

The incoming and outgoing waves in leads $\mathrm{S_L}$ and $\mathrm{S_R}$ can be described in the following basis

$$a_\mathrm{S}^\mathrm{in} \equiv \left[\hat{\mathrm{a}}_e(\mathrm{S_L}), \hat{\mathrm{a}}_e(\mathrm{S_R}), \hat{\mathrm{a}}_h(\mathrm{S_L}), \hat{\mathrm{a}}_h(\mathrm{S_R})\right]^\mathrm{T}, \tag{C.7}$$

$$b_\mathrm{S}^\mathrm{out} \equiv \left[\hat{\mathrm{b}}_e(\mathrm{S_L}), \hat{\mathrm{b}}_e(\mathrm{S_R}), \hat{\mathrm{b}}_h(\mathrm{S_L}), \hat{\mathrm{b}}_h(\mathrm{S_R})\right]^\mathrm{T}. \tag{C.8}$$

Rearranging Eq. (C.6) in the order of incoming and outgoing states gives

$$\left(\begin{bmatrix} e^{-i\varphi/2} & 0 & 0 & 0 \\ 0 & e^{-i\varphi/2} & 0 & 0 \\ 0 & 0 & e^{i\varphi/2} & 0 \\ 0 & 0 & 0 & e^{i\varphi/2} \end{bmatrix} - \sin\alpha S_{\mathrm{N}} \begin{bmatrix} 0 & 0 & e^{-i\varphi/2} & 0 \\ 0 & 0 & 0 & e^{-i\varphi/2} \\ e^{i\varphi/2} & 0 & 0 & 0 \\ 0 & e^{i\varphi/2} & 0 & 0 \end{bmatrix}\right) b_{\mathrm{S}}^{\mathrm{out}}$$
$$= \left(S_{\mathrm{N}} \begin{bmatrix} e^{-i\varphi/2} & 0 & 0 & 0 \\ 0 & e^{-i\varphi/2} & 0 & 0 \\ 0 & 0 & e^{i\varphi/2} & 0 \\ 0 & 0 & 0 & e^{i\varphi/2} \end{bmatrix} - \sin\alpha \begin{bmatrix} 0 & 0 & e^{-i\varphi/2} & 0 \\ 0 & 0 & 0 & e^{-i\varphi/2} \\ e^{i\varphi/2} & 0 & 0 & 0 \\ 0 & e^{i\varphi/2} & 0 & 0 \end{bmatrix}\right) a_{\mathrm{S}}^{\mathrm{in}}. \tag{C.9}$$

After some algebra we have

$$\left(1 - \sin\alpha S_{\mathrm{N}} \begin{bmatrix} 0 & r_A \\ r_A^\star & 0 \end{bmatrix}\right) b_{\mathrm{S}}^{\mathrm{out}} = \left(S_{\mathrm{N}} - \sin\alpha \begin{bmatrix} 0 & r_A \\ r_A^\star & 0 \end{bmatrix}\right) a_{\mathrm{S}}^{\mathrm{in}}, \tag{C.10}$$

where

$$r_A \equiv \begin{bmatrix} e^{i\varphi/2}\mathbf{1} & \mathbf{0} \\ \mathbf{0} & e^{-i\varphi/2}\mathbf{1} \end{bmatrix} \tag{C.11}$$

originates from Andreev reflection. We define matrix

$$M = \sin\alpha \begin{bmatrix} 0 & r_A \\ r_A^\star & 0 \end{bmatrix}. \tag{C.12}$$

Using this we write Eq. (C.10) in the following form

$$b_{\mathrm{S}}^{\mathrm{out}} = (\mathbf{1} - M)^{-1}(\mathbf{1} - M^\dagger) S_{\mathrm{N}} a_{\mathrm{S}}^{\mathrm{in}}. \tag{C.13}$$

Here we have the scattering matrix of SNS junction

$$S_{\mathrm{SNS}} = (\mathbf{1} - M)^{-1}(\mathbf{1} - M^\dagger) S_{\mathrm{N}}. \tag{C.14}$$

The scattering matrix of the normal region does not couple electrons and holes, therefore the matrix S_{N} has block-diagonal form

$$S_{\mathrm{N}} = \begin{bmatrix} s_0(\varepsilon) & 0 \\ 0 & s_0(-\varepsilon)^\dagger \end{bmatrix}. \tag{C.15}$$

Substituting Eq. (C.15) in (C.14) gives

$$S_{\mathrm{SNS}} = \begin{bmatrix} \mathcal{A}^{-1} & \sin\alpha\, \mathcal{A}^{-1} s_0 r_A \\ \sin\alpha\, s_0^\dagger r_A^\star \mathcal{A}^{-1} & 1 + (\sin\alpha)^2 s_0^\dagger r_A^\star \mathcal{A}^{-1} s_0 r_A \end{bmatrix}$$
$$\times \begin{bmatrix} s_0 & -\sin\alpha r_A \\ -\sin\alpha r_A^\star & s_0^\dagger \end{bmatrix}. \tag{C.16}$$

with

$$\mathcal{A}^{-1} \equiv \left[1 - (\sin\alpha)^2 s_0 r_A s_0^\dagger r_A^\star\right]^{-1} \tag{C.17}$$

Using the polar decomposition [23], the matrix $s_0(\varepsilon)$ can be written in terms of transmission matrix $\mathbf{D} = \mathrm{diag}(D_1, D_2, ..., D_N)$ that is a $N \times N$ diagonal matrix of transmission eigenvalues of normal region

$$s_0(\varepsilon) = \begin{bmatrix} U_1 & \mathbf{0} \\ \mathbf{0} & U_2 \end{bmatrix} \begin{bmatrix} \sqrt{1-\mathbf{D}} & \sqrt{\mathbf{D}} \\ \sqrt{\mathbf{D}} & -\sqrt{1-\mathbf{D}} \end{bmatrix} \begin{bmatrix} V_1 & \mathbf{0} \\ \mathbf{0} & V_2 \end{bmatrix} \tag{C.18}$$

where U_1, U_2, V_1, V_2 are four $N \times N$ unitary matrices. Inserting Eq. (C.18) into $\mathcal{A}^{-1}$, Eq. (C.17), gives

$$\mathcal{A}^{-1} = \tag{C.19}$$
$$\begin{bmatrix} U_1[1-(\sin\alpha)^2(1-\mathbf{D}+e^{-i\varphi}\mathbf{D})]U_1^\dagger & U_1(\sin\alpha)^2(1-e^{i\varphi})\mathbf{D}^{1/2}(1-\mathbf{D})^{1/2}U_2^\dagger \\ U_2(\sin\alpha)^2(e^{-i\varphi}-1)\mathbf{D}^{1/2}(1-\mathbf{D})^{1/2}U_1^\dagger & U_2[1-(\sin\alpha)^2(1-\mathbf{D}+e^{i\varphi}\mathbf{D})]U_2^\dagger \end{bmatrix}^{-1}.$$

To inverse the matrix in Eq. (C.19) we use block matrix inversion formula. If a matrix is partitioned into four blocks, it can be inverted as follows

$$\begin{bmatrix} A & B \\ C & D \end{bmatrix}^{-1} = \begin{bmatrix} A^{-1} + A^{-1}B(D-CA^{-1}B)^{-1}CA^{-1} & -A^{-1}B(D-CA^{-1}B)^{-1} \\ -(D-CA^{-1}B)^{-1}CA^{-1} & (D-CA^{-1}B)^{-1} \end{bmatrix}. \tag{C.20}$$

Following Eq. (C.20) we have the inverse of the matrix in Eq. (C.19)

$$(1-(\sin\alpha)^2 s_0 r_A s_0^\dagger r_A^\star)^{-1} = \begin{bmatrix} U_1 Q_1 U_1^\dagger & U_1 Q_2 U_2^\dagger \\ U_2(-Q_2)U_1^\dagger & U_2 Q_3 U_2^\dagger \end{bmatrix}, \tag{C.21}$$

Where

$$\begin{aligned} Q_1 =& [1-(\sin\alpha)^2(1+(e^{-i\varphi}-1)\mathbf{D})]^{-1} \\ & [1+2(\sin\alpha)^4(\cos\varphi-1)\mathbf{D}(1-\mathbf{D})[1+(\sin\alpha)^4-2(\sin\alpha)^2(1+(\cos\varphi-1)\mathbf{D})]^{-1}] \end{aligned} \tag{C.22}$$

$$Q_2 = (\sin\alpha)^2(e^{i\varphi}-1)\mathbf{D}^{1/2}(1-\mathbf{D})^{1/2}[1+(\sin\alpha)^4-2(\sin\alpha)^2(1+(\cos\varphi-1)\mathbf{D})]^{-1}$$
$$Q_3 = [1-(\sin\alpha)^2(1+(e^{-i\varphi}-1)\mathbf{D})][1+(\sin\alpha)^4-2(\sin\alpha)^2(1+(\cos\varphi-1)\mathbf{D})]^{-1}.$$

Substituting Eqs.(C.22) in (C.16) gives the scattering matrix of SNS junction as the multiplication of following matrices

$$
\begin{aligned}
S_{\mathrm{SNS}} = \Bigg[\Bigg[&\Big(U_1 Q_1 U_1^{\dagger}\Big), \Big(U_1 Q_2 U_2^{\dagger}\Big), \Big(U_1 \sin\alpha e^{i\varphi/2}[Q_1(1-\mathbf{D})^{1/2} + Q_2\mathbf{D}^{1/2}]V_1\Big), \\
&\Big(U_1 \sin\alpha e^{-i\varphi/2}[Q_1\mathbf{D}^{1/2} - Q_2(1-\mathbf{D})^{1/2}]V_2\Big)\Bigg]; \\
\Bigg[&\Big(U_2(-Q_2)U_1^{\dagger}\Big), \Big(U_2 Q_3 U_2^{\dagger}\Big), \Big(U_2 \sin\alpha e^{i\varphi/2}[-Q_2(1-\mathbf{D})^{1/2} + Q_3\mathbf{D}^{1/2}]V_1\Big), \\
&\Big(U_2 \sin\alpha e^{-i\varphi/2}[-Q_2\mathbf{D}^{1/2} - Q_3(1-\mathbf{D})^{1/2}]V_2\Big)\Bigg]; \\
\Bigg[&\Big(V_1^{\dagger} \sin\alpha[e^{-i\varphi/2}Q_1(1-\mathbf{D})^{1/2} - e^{i\varphi/2}Q_2\mathbf{D}^{1/2}]U_1^{\dagger}\Big), \\
&\Big(V_1^{\dagger} \sin\alpha[e^{-i\varphi/2}Q_2(1-\mathbf{D})^{1/2} + e^{i\varphi/2}Q_3\mathbf{D}^{1/2}]U_2^{\dagger}\Big), \\
&\Big(V_1^{\dagger}[1 + (\sin\alpha)^2\Big(Q_1(1-\mathbf{D}) + e^{i\varphi}Q_3\mathbf{D} + (1-e^{i\varphi})Q_2\mathbf{D}^{1/2}(1-\mathbf{D})^{1/2}\Big)]V_1\Big), \\
&\Big(V_1^{\dagger}(\sin\alpha)^2[(e^{-i\varphi}Q_1 - Q_3)\mathbf{D}^{1/2}(1-\mathbf{D})^{1/2} - Q_2(\mathbf{D} + e^{-i\varphi}(1-\mathbf{D}))]V_2\Big)\Bigg]; \\
\Bigg[&\Big(V_2^{\dagger} \sin\alpha[e^{-i\varphi/2}Q_1\mathbf{D}^{1/2} + e^{i\varphi/2}Q_2(1-\mathbf{D})^{1/2}]U_1^{\dagger}\Big), \\
&\Big(V_2^{\dagger} \sin\alpha[e^{-i\varphi/2}Q_2\mathbf{D}^{1/2} - e^{i\varphi/2}Q_3(1-\mathbf{D})^{1/2}]U_2^{\dagger}\Big), \\
&\Big(V_2^{\dagger}(\sin\alpha)^2[(Q_1 - e^{i\varphi}Q_3)\mathbf{D}^{1/2}(1-\mathbf{D})^{1/2} - Q_2(\mathbf{D} + e^{i\varphi}(1-\mathbf{D}))]V_1\Big), \\
&\Big(V_2^{\dagger}[1 + (\sin\alpha)^2\Big(e^{-i\varphi}Q_1\mathbf{D} + Q_3(1-\mathbf{D}) - (1+e^{-i\varphi})Q_2\mathbf{D}^{1/2}(1-\mathbf{D})^{1/2}\Big)]V_2\Big)\Bigg]\Bigg] \\
\times &\begin{bmatrix}
U_1(1-\mathbf{D})^{1/2}V_1 & U_1\mathbf{D}^{1/2}V_2 & -\sin\alpha e^{i\varphi/2} & \mathbf{0} \\
U_2\mathbf{D}^{1/2}V_1 & -U_2(1-\mathbf{D})^{1/2}V_2 & \mathbf{0} & -\sin\alpha e^{-i\varphi/2} \\
-\sin\alpha e^{-i\varphi/2} & \mathbf{0} & V_1^{\dagger}(1-\mathbf{D})^{1/2}U_1^{\dagger} & V_1^{\dagger}\mathbf{D}^{1/2}U_2^{\dagger} \\
\mathbf{0} & -\sin\alpha e^{i\varphi/2} & V_2^{\dagger}\mathbf{D}^{1/2}U_1^{\dagger} & -V_2^{\dagger}(1-\mathbf{D})^{1/2}U_2^{\dagger}
\end{bmatrix}.
\end{aligned}
\tag{C.23}
$$

The elements of the matrix in Eq. (C.23) represents the following scatterings

$$
S_{\mathrm{SNS}} = \begin{bmatrix}
r_{ee} & t'_{ee} & r_{eh} & t'_{eh} \\
t_{ee} & r'_{ee} & t_{eh} & r'_{eh} \\
r_{he} & t'_{he} & r_{hh} & t'_{hh} \\
t_{he} & r'_{he} & t_{hh} & r'_{hh}
\end{bmatrix}. \tag{C.24}
$$

Therefore we have the following amplitudes from Eq. (C.23)

$$\begin{aligned}\mathcal{D}_n^{ee}(E) =&(1-(\sin\alpha)^2)^2 D_n(1+(\sin\alpha)^4-2(\sin\alpha)^2\cos\varphi)\\ &[((\sin\alpha)^2-1)^2-2(\sin\alpha)^2 D_n(\cos\varphi-1)]^{-2},\\ \mathcal{D}_n^{eh}(E) =&2(\sin\alpha)^2(1-(\sin\alpha)^2)^2 D_n(1-D_n)(1-\cos\varphi)\\ &[((\sin\alpha)^2-1)^2-2(\sin\alpha)^2 D_n(\cos\varphi-1)]^{-2}.\end{aligned} \tag{C.25}$$

Results in Eq. (C.25) are in the agreement with the single channel amplitudes.

Full expressions for transmission amplitudes when the left and right superconductors are nonsimilar, are

$$\begin{aligned}\mathcal{D}_n^{ee}(E) =&D_n\cos^2(\alpha_{\mathrm{L}})\cos^2(\alpha_{\mathrm{R}})[1+\sin^2(\alpha_{\mathrm{L}})\sin^2(\alpha_{\mathrm{R}})-2\sin(\alpha_{\mathrm{L}})\sin(\alpha_{\mathrm{R}})\cos\varphi]\\ &(\cos^2(\alpha_{\mathrm{L}})\cos^2(\alpha_{\mathrm{R}})+D_n[\sin^2(\alpha_{\mathrm{L}})+\sin^2(\alpha_{\mathrm{R}})-2\sin(\alpha_{\mathrm{L}})\sin(\alpha_{\mathrm{R}})\cos\varphi])^{-2},\\ \mathcal{D}_n^{eh}(E) =&D_n(1-D_n)\cos^2(\alpha_{\mathrm{L}})\cos^2(\alpha_{\mathrm{R}})[\sin^2(\alpha_{\mathrm{L}})+\sin^2(\alpha_{\mathrm{R}})-2\sin(\alpha_{\mathrm{L}})\sin(\alpha_{\mathrm{R}})\cos\varphi]\\ &(\cos^2(\alpha_{\mathrm{L}})\cos^2(\alpha_{\mathrm{R}})+D_n[\sin^2(\alpha_{\mathrm{L}})+\sin^2(\alpha_{\mathrm{R}})-2\sin(\alpha_{\mathrm{L}})\sin(\alpha_{\mathrm{R}})\cos\varphi])^{-2}.\end{aligned} \tag{C.26}$$

And adding these two transmission gives

$$\mathcal{D}_n^{e}(E) = 2D_n\xi_{\mathrm{L}}\xi_{\mathrm{R}}\frac{D_n\xi_{\mathrm{L}}\xi_{\mathrm{R}}+(2-D_n)(E^2-\Delta_{\mathrm{L}}\Delta_{\mathrm{R}}\cos\varphi)}{((2-D_n)\xi_{\mathrm{L}}\xi_{\mathrm{R}}+D_n(E^2-\Delta_{\mathrm{L}}\Delta_{\mathrm{R}}\cos\varphi))^2}. \tag{C.27}$$

References

[1] F. Giazotto, T. T. Heikkilä, A. Luukanen, A. M. Savin, and J. P. Pekola, "Opportunities for mesoscopics in thermometry and refrigeration: Physics and applications", Rev. Mod. Phys. **78**, 217–274 (2006) (cit. on p. 1).

[2] K. Maki and A. Griffin, "Entropy Transport Between Two Superconductors by Electron Tunneling", Phys. Rev. Lett. **15**, 921–923 (1965) (cit. on pp. 1, 2, 4, 7, 22, 24).

[3] J. T. Muhonen, M. Meschke, and J. P. Pekola, "Micrometre-scale refrigerators", Rep. Prog. Phys. **75**, 046501 (2012) (cit. on p. 1).

[4] M. J. Martínez-Pérez and F. Giazotto, "Efficient phase-tunable Josephson thermal rectifier", Appl. Phys. Lett. **102**, 182602 (2013) (cit. on p. 1).

[5] M. José Martínez-Pérez and F. Giazotto, "A quantum diffractor for thermal flux", Nat. Commun. **5**, 3579 (2014) (cit. on p. 1).

[6] G. D. Guttman, E. Ben-Jacob, and D. J. Bergman, "Interference effect heat conductance in a Josephson junction and its detection in an rf SQUID", Phys. Rev. B **57**, 2717–2719 (1998) (cit. on pp. 1, 2).

[7] E. Zhao, T. Löfwander, and J. A. Sauls, "Phase Modulated Thermal Conductance of Josephson Weak Links", Phys. Rev. Lett. **91**, 077003 (2003) (cit. on pp. 1, 2, 7, 24).

[8] E. Zhao, T. Löfwander, and J. A. Sauls, "Heat transport through Josephson point contacts", Phys. Rev. B **69**, 134503 (2004) (cit. on pp. 1, 2, 7, 24, 25).

[9] F. Giazotto and M. J. Martínez-Pérez, "The Josephson heat interferometer", Nature **492**, 401 (2012) (cit. on pp. 1, 2, 4, 7, 19, 38).

[10] A. Fornieri and F. Giazotto, "Towards phase-coherent caloritronics in superconducting circuits", Nat. Nanotechnol. **12**, 944 (2017) (cit. on pp. 1, 5).

[11] H. Q. Nguyen, T. Aref, V. J. Kauppila, M. Meschke, C. B. Winkelmann, H. Courtois, and J. P. Pekola, "Trapping hot quasi-particles in a high-power superconducting electronic cooler", New J. Phys. **15**, 085013 (2013) (cit. on p. 2).

[12] S. Juergens, F. Haupt, M. Moskalets, and J. Splettstoesser, "Thermoelectric performance of a driven double quantum dot", Phys. Rev. B **87**, 245423 (2013) (cit. on p. 3).

[13] D. Venturelli, R. Fazio, and V. Giovannetti, "Minimal Self-Contained Quantum Refrigeration Machine Based on Four Quantum Dots", Phys. Rev. Lett. **110**, 256801 (2013) (cit. on p. 3).

[14] R. Uzdin, A. Levy, and R. Kosloff, "Equivalence of Quantum Heat Machines, and Quantum-Thermodynamic Signatures", Phys. Rev. X **5**, 031044 (2015) (cit. on p. 3).

[15] A. Majumdar, "Thermoelectricity in Semiconductor Nanostructures", Science **303**, 777–778 (2004) (cit. on p. 3).

[16] G. J. Snyder and E. S. Toberer, "Complex thermoelectric materials", Nat. Mater. **7**, 105 (2008) (cit. on p. 3).

[17] Y. Dubi and M. Di Ventra, "Colloquium: Heat flow and thermoelectricity in atomic and molecular junctions", Rev. Mod. Phys. **83**, 131–155 (2011) (cit. on p. 3).

[18] A. Fornieri, G. Timossi, R. Bosisio, P. Solinas, and F. Giazotto, "Negative differential thermal conductance and heat amplification in superconducting hybrid devices", Phys. Rev. B **93**, 134508 (2016) (cit. on p. 3).

[19] Prof. Dr. J. Clarke and Prof. Dr. A. I. Braginski, *The SQUID Handbook* (2005) (cit. on p. 3).

[20] B. D. Josephson, "Possible new effects in superconductive tunnelling", Physics Letters **1**, 251–253 (1962) (cit. on p. 4).

[21] A. F. Andreev, "The thermal conductivity of the intermediate state in superconductors", JETP **19**, [Online; accessed 13. Nov. 2018], 1228 (1964) (cit. on p. 4).

[22] S. Spilla, F. Hassler, A. Napoli, and J. Splettstoesser, "Dephasing due to quasiparticle tunneling in fluxonium qubits: a phenomenological approach", New J. Phys. **17**, 065012 (2015) (cit. on pp. 5, 24).

[23] C. W. J. Beenakker, "Random-matrix theory of quantum transport", (cit. on pp. 5, 7, 11, 19, 22, 29, 33, 52).

[24] P. A. Lee and A. D. Stone, "Universal Conductance Fluctuations in Metals", Phys. Rev. Lett. **55**, 1622–1625 (1985) (cit. on pp. 6, 19).

[25] B. L. Altshuler, "Fluctuations in the extrinsic conductivity of disordered conductors ", JETP **41**, 648 (1985) (cit. on pp. 6, 19).

[26] B. L. Altshuler, P. A. Lee, and W. R. Webb, *Mesoscopic Phenomena in Solids, Volume 30* (North Holland, 1991) (cit. on pp. 6, 19).

[27] Y. Imry, "Active Transmission Channels and Universal Conductance Fluctuations", EPL **1**, 249 (1986) (cit. on p. 6).

[28] R. Landauer, "Spatial Variation of Currents and Fields Due to Localized Scatterers in Metallic Conduction", IBM J. Res. Dev. **1**, 223–231 (1957) (cit. on p. 7).

[29] R. Landauer, "Electrical transport in open and closed systems", Z. Phys. B: Condens. Matter **68**, 217–228 (1987) (cit. on p. 7).

[30] M. Büttiker, "Four-Terminal Phase-Coherent Conductance", Phys. Rev. Lett. **57**, 1761–1764 (1986) (cit. on p. 7).

[31] H. Fukuyama and T. Ando, *Transport Phenomena in Mesoscopic Systems | SpringerLink* (Springer, Berlin, Heidelberg, 1992) (cit. on p. 7).

[32] P. N. Butcher, "Thermal and electrical transport formalism for electronic microstructures with many terminals", J. Phys.: Condens. Matter **2**, 4869 (1990) (cit. on p. 8).

[33] Y. V. Nazarov and Y. M. Blanter, *Quantum transport: introduction to nanoscience* (Cambridge University Press, 2009) (cit. on pp. 10, 26).

[34] *Introduction to Superconductivity: Second Edition*, [Online; accessed 25. Oct. 2018], 2018 (cit. on p. 14).

[35] C. Poole, H. Farach, R. Creswick, and R. Prozorov, *Superconductivity* (Academic Press, 2007) (cit. on pp. 14, 17).

[36] C. W. J. Beenakker, "Universal limit of critical-current fluctuations in mesoscopic Josephson junctions", Phys. Rev. Lett. **67**, 3836–3839 (1991) (cit. on p. 19).

[37] C. W. J. Beenakker, "Three "Universal" Mesoscopic Josephson Effects", SpringerLink, 235–253 (1992) (cit. on pp. 21, 32).

[38] S. Spilla, F. Hassler, and J. Splettstoesser, "Measurement and dephasing of a flux qubit due to heat currents", New J. Phys. **16**, 045020 (2014) (cit. on p. 24).

[39] J. B. Pendry, *The scattering of positrons at surfaces*, [Online; accessed 22. Nov. 2018], 1983 (cit. on p. 24).

[40] S. Jezouin, F. D. Parmentier, A. Anthore, U. Gennser, A. Cavanna, Y. Jin, and F. Pierre, "Quantum Limit of Heat Flow Across a Single Electronic Channel", Science **342**, 601–604 (2013) (cit. on p. 24).

[41] O. N. Dorokhov, "On the coexistence of localized and extended electronic states in the metallic phase", Solid State Commun. **51**, 381–384 (1984) (cit. on p. 25).

[42] P. A. Mello and J.-L. Pichard, "Maximum-entropy approaches to quantum electronic transport", Phys. Rev. B **40**, 5276–5278 (1989) (cit. on p. 25).

[43] O. Dorokhov, "Transmission coefficient and the localization length of an electron in N bound disordered chains", JETP Lett **36**, 318–321 (1982) (cit. on p. 27).

[44] P. A. Mello, P. Pereyra, and N. Kumar, "Macroscopic approach to multichannel disordered conductors", Ann. Phys. **181**, 290–317 (1988) (cit. on p. 27).

[45] E. Akkermans, P. E. Wolf, and R. Maynard, "Coherent Backscattering of Light by Disordered Media: Analysis of the Peak Line Shape", Phys. Rev. Lett. **56**, 1471–1474 (1986) (cit. on p. 27).

[46] M. Cahay, M. McLennan, and S. Datta, "Conductance of an array of elastic scatterers: A scattering-matrix approach", Phys. Rev. B **37**, 10125–10136 (1988) (cit. on p. 27).

[47] N. Giordano, "Experimental study of localization in thin wires", Phys. Rev. B **22**, 5635–5654 (1980) (cit. on p. 27).

[48] C. W. J. Beenakker and B. Rejaei, "Nonlogarithmic repulsion of transmission eigenvalues in a disordered wire", Phys. Rev. Lett. **71**, 3689–3692 (1993) (cit. on pp. 27, 29).

[49] T. W. Larsen, K. D. Petersson, F. Kuemmeth, T. S. Jespersen, P. Krogstrup, J. Nygård, and C. M. Marcus, "Semiconductor-Nanowire-Based Superconducting Qubit", Phys. Rev. Lett. **115**, 127001 (2015) (cit. on p. 27).

[50] G. E. Blonder, M. Tinkham, and T. M. Klapwijk, "Transition from metallic to tunneling regimes in superconducting microconstrictions: Excess current, charge imbalance, and supercurrent conversion", Phys. Rev. B **25**, 4515–4532 (1982) (cit. on p. 32).

[51] C. B. Satterthwaite, "Thermal Conductivity of Normal and Superconducting Aluminum", Phys. Rev. **125**, 873–876 (1962) (cit. on p. 34).

[52] A. C. Anderson and S. G. O'Hara, "The lattice thermal conductivity of normal and superconducting niobium", J. Low Temp. Phys. **15**, 323–333 (1974) (cit. on p. 35).

[53] S. Belin and K. Behnia, "Thermal Conductivity of Superconducting $(TMTSF)_2ClO_4$: Evidence for a Nodeless Gap", Phys. Rev. Lett. **79**, 2125–2128 (1997) (cit. on p. 35).

[54] P. Virtanen and F. Giazotto, "Fluctuation of heat current in Josephson junctions", AIP Adv. **5**, 027140 (2015) (cit. on p. 39).